UCID-20614

A Geostatistical (Kriging) Study of Geological and Gas Production Data from West Virginia

N. Mao

Prepared for
Morgantown Energy Technology Center
Morgantown, WV

January, 1986

Lawrence Livermore National Laboratory

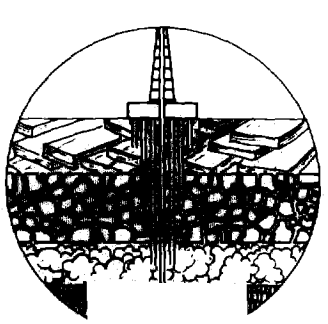

Unconventional Gas Program

Eastern Devonian Shales Research

Printed in the United States of America
Available from
National Technical Information Service
U.S. Department of Commerce
5285 Port Royal Road
Springfield, VA 22161

Price Code	Page Range
A01	Microfiche
Papercopy Prices	
A02	001 - 050
A03	051 - 100
A04	101 - 200
A05	201 - 300
A06	301 - 400
A07	401 - 500
A08	501 - 600
A09	601

INDEX

ABSTRACT

As part of the Unconventional Gas Program/Eastern Devonian shale research, we carried out geostatistical (kriging) analyses of geological and gas production data from southwestern West Virginia. The geological parameters studied consist of the top and bottom elevations of the Greenbrier limestone and Berea sandstone, the bottom elevation of the Devonian shale, and the thickness of the Greenbrier and Berea. The production data consist of rock pressure and ten year cumulative production. No gross correlation between the geological and production data is obvious. However we note that low values of ten year cumulative production are generally found in the vicinity of the Warfield anticline while high values of ten-year cumulative production are located in the NW limb of the anticline. Both rock pressure and ten year cumulative production can be reasonably estimated within the study area.

1. INTRODUCTION

Thousands of wells have been drilled in the Eastern Devonian shales. The data collected from these wells form a database in which we may find some clues to the pattern of production. This in turn would help to plan future drilling strategy in the same or nearby fields. One approach is to carry out statistical analyses of the geological and production data. The method of analysis should be capable of recognizing the spatial correlations that may exist in the data. Kriging is such a technique. It is currently used at LLNL, in support of the Nuclear Test Program (Mao, 1983). This report demonstrates the application of kriging to a particular Devonian Shale database: that from Columbia Gas System Service Corporation. This research is part of the Unconventional Gas Program at LLNL (Heuze, 1986).

2. PRINCIPLES OF KRIGING

Kriging is a statistical spatial estimation technique. It was named after D. G. Krige who originally applied the idea to the estimation of ore reserves in gold mines. The mathematical foundations of kriging were developed by Matheron (1971) and are described in the book by Journel and Huijbregts (1978). Kriging consists of two parts: estimation of a variogram (or semi-variogram) which describes the degree of correlation between any two observations as a function of the distance between them, and calculation of the kriging weights which indicate the relative influence of each data observation on the interpolations. A kriging estimate has two optimal statistical properties. First, it is unbiased, i.e. it reproduces the data value if there is no measurement error. Second, the kriging estimate is of minimum variance. Therefore, kriging may be considered as a weighted least-squares technique where the weights are calculated by minimizing the variance under the constraint of unbiasedness, using the Lagrangian multiplier technique.

The variogram shows the relation between variance and distance for the data. The variance of a set of data separated by a given distance is defined as the square of the standard deviation of that set. By choosing a variogram for a data set, we tailor the kriging process to that specific data set. Kriging was designed under certain assumptions to produce estimates that

minimize the difference between the true surface and the estimated surface for the whole region, not just at data points. This is because the optimum kriging weights depend only on the location of the data and the form of the variogram, not on the measured values themselves. In addition to the estimates, kriging provides the standard deviation of the error, which is a measure of the uncertainty of the estimates.

In kriging, the observed value of the phenomenon is generally separated into two parts, i.e., a large scale trend called drift and a small scale fluctuation of the residuals which the variogram tries to model. Figure 1 shows the variance plotted as a function of distance between two data points; this is a common presentation of the variogram. The parameters a and w are called range and sill. The range is the range of influence between two data points and the sill is the maximum variability in the system. The nugget effect (c) is a parameter which indicates a discontinuity at zero distance as in a gold mine where a gold nugget may be found at one place but not next to it. A nested structure indicates that the variogram may be represented by more than one simple model. For example, a nested spherical model may consist of two simple spherical models with different ranges and sills. At short distance, the observed variability depends on the short range model only,

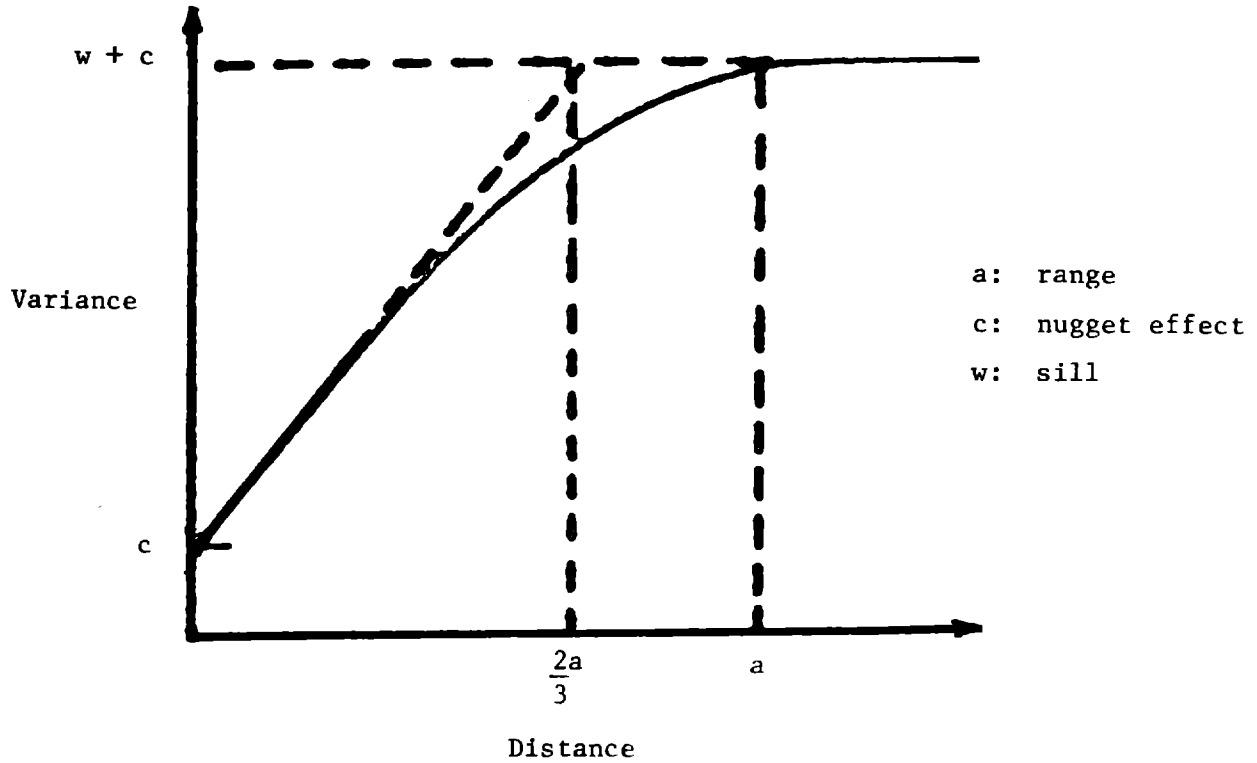

Figure 1: Spherical Variogram Model.

while for large distance it will depend on both models (see Figure 3 for example). Not all variogram models have a sill. A linear variogram may extend indefinitely. However, short distance behavior of a variogram is much more important than behavior at large distances because nearby data always have more influence on the estimates than distant data.

The kriging estimate at any location is a linear combination of the weighted average of surrounding data. A kriged contour map of a parameter is produced in two steps. First, we estimate the values of the parameter on the nodes of a regular grid, using kriging. Then we contour the map based on the kriged values at the grid nodes (see Fig. 4 for example). The smoothness of the contour line is controlled by the contour routine. However, the accuracy of the contoured values is controlled by the estimation technique. Since kriging is the best linear unbiased estimator, a kriged map is the most accurate map in that category. An uncertainty contour map is produced in a similar fashion. Here the values of the one standard deviation of the estimate are calculated and contoured. By using these maps we can find out both the estimate at any location and how good the estimate is. If the estimation uncertainty has a normal distribution, then we expect that 95.5% of the estimates will be within ± of two standard deviations (see Fig. 6 for example).

Once we have identified the variogram and the drift and have calculated the kriging estimates and their associated uncertainties, we have to find a way to validate the model. The validation process is called Doubting Thomas. We remove one data point at a time and try to estimate the value and its associated uncertainty at the point, using the rest of the data. We repeat the process for all data points and make statistical analyses of the results. Three criteria are used:

$$\sum_{i=1}^{N} [(z^*(x_i) - z(x_i)] \simeq 0,$$

$$\sum_{i=1}^{N} [(z^*(x_i) - z(x_i)]^2 \text{ is minimum,} \qquad (1)$$

and

$$\sum_{i=1}^{N} \left[\frac{z^*(x_i) - z(x_i)}{s^*(x_i)}\right]^2 \simeq 1$$

where $z(x_i)$, $z^*(x_i)$, and $s^*(x_i)$ are respectively the measured and estimated values, and the estimated uncertainties at location x_i for the N data points.

The first criterion says that the kriged average error should be close to zero (unbiased). The second criterion says that the mean squared error should be at a minimum (optimal). The ratio of the kriged error and the uncertainty is called the standard error. If a model is good, the calculated uncertainty should reflect the calculated error, thus the ratio should be close to 1.

A scatter diagram can be plotted between measured and estimated values from the Thomas validation process (see Fig. 8 for example). If the estimates are perfect, then all points should fall on a straight diagonal line.

In addition to the overall consistency between the model and the data, we should also look for any local inconsistency. If the absolute value of the standard error for a particular data point is larger than 2.5, then we should double-check that point. It is quite possible that the data point is bad or that some local discontinuity, such as a fault, is in the vicinity.

3. ANALYSIS OF GEOLOGICAL DATA

Recent effort by the BDM Corporation and the Gas Research Institute (GRI) have resulted in a database called the Eastern Gas Data System (EGDS). It is designed to provide data on Devonian shale gas wells for research, exploration, and development efforts. It includes data pertaining to well location, drilling, completion, stimulation, production history, and other pertinent geological and technical information. However we did not use data from this database because its format was being changed during our study period.

The data used for this study were supplied by Morgantown Energy Technology Center (METC) from the Columbia Gas System Service Corporation's eastern gas shale database with corrections to well locations by EG&G Washington Analytical Services Center, Inc.. There are 617 wells in the study area, which includes part of Lincoln, Logan, Mingo, and Wayne counties. Since all the geological contacts are expressed as depths from the surface while the surface elevations at well locations range from 580 ft to 1580 ft above sea level, we converted all depth data to either elevation or thickness first so that all data have a common reference. Only the converted geological data were used in the present study. In all figures, the distance was expressed in unit of degree multiplied by 1000. Furthermore we changed the sign of longitude in order to have correct map orientation. For elevation, negative value means that it is below sea level.

3.1 Greenbrier Limestone

There are 612 data points of the Greenbrier top and bottom elevations in the study area. Figure 2 shows the locations of the data. The top of the Greenbrier ranges from 315 ft to 812 ft below sea level and the bottom ranges from 497 ft to 1012 ft. The thickness is between 96 ft and 267 ft. The variogram of the residual of a linear drift for both the top and the bottom of the Greenbrier can be modeled by a nested spherical variogram, such as defined in Chapter 2. Figure 3 shows the variogram of the bottom elevation. The two ranges are 60 and 160 units respectively. No correlation is observed beyond a distance of 160 units. There is also a small nugget effect of 300 ft^2 which is most likely due to the uncertainty in the data. The kriged contour maps for

the top and the bottom of the Greenbrier are shown in Figures 4 and 5. The two maps are very similar. The general trend of the structure is in a direction of N60°E. The long narrow trough in the northwestern part of the maps corresponds to the Guthrie syncline and the ridge in the south and southeastern corner corresponds to the Warfield anticline. These maps are also very similar to a map entitled "Structure Contour Map Datum Greenbrier Limestone in West Virginia" by Haught (1968).

Figures 6 and 7 show the uncertainty of the estimates for the top and bottom elevations. Figures 8 and 9 are scatter plots of measured versus estimated values. These figures indicate that in general the estimated elevations for both the top and the bottom of the Greenbrier are quite consistent with those measured.

The kriged thickness map for the Greenbrier is shown in Figure 10. In general the thickness in NW and SE quadrants is greater than that in the NE and SW regions.

3.2 Berea Sandstone

There are 607 data points for the Berea sandstone in the study area. The elevation of the top of the Berea ranges from 1578 ft to 1027 ft below sea level. The elevation of the bottom ranges from 1593 ft to 1042 ft below sea level. The kriged contour maps for the top and bottom are shown in Figures 11 and 12 which are very similar to those for the Greenbrier. Therefore the geological structure in the study area does not vary much with depth. The thickness of the Berea is generally smaller than 25 ft for most of the study area except in the SW corner where thicknesses lager than 100 ft are intermixed with much thinner beds. We suspect that some data in the SW corner may be in error. The thickness of the Berea as shown in Figure 13 is the kriged results after extensive deleting of the "outliers".

3.3 Devonian Shale

The database shows 537 wells reaching the bottom of the Devonian shale. However some of the data in fact represent the depth where drilling stopped. Therefore the true bottom depths of the shale at those locations may be deeper

than what the data indicate. Figure 14 shows the variogram of the residuals from a linear drift. The fitted model has a large nugget effect (2000 ft^2) and a nested spherical model. The results of validation from this model indicated that 24 data points had a standard error (see section 3) outside the bounds of -2.5 to 2.5. Furthermore 21 of the 24 standard errors were negative. Since a negative value implies that the estimated depths are deeper than the data values, it is conceivable that these 21 data are from wells which never reached the bottom of the Devonian shale. With this assumption, we removed these 21 data from the database and analyzed the elevations again. Figure 15 shows the variogram of the residuals from a linear drift for the remain 516 data. The nugget effect is reduced to 700 ft^2 and a simple spherical model with a range of 100 units can be fitted.

The kriged contour map for the bottom of the Devonian shale is shown in Figure 16. Again, the basic structure is very similar to those shown before. The uncertainty map and the scatter plot for the bottom of the Devonian shale are shown in Figures 17 and 18 respectively. In general the estimated elevations are quite consistent with those measured.

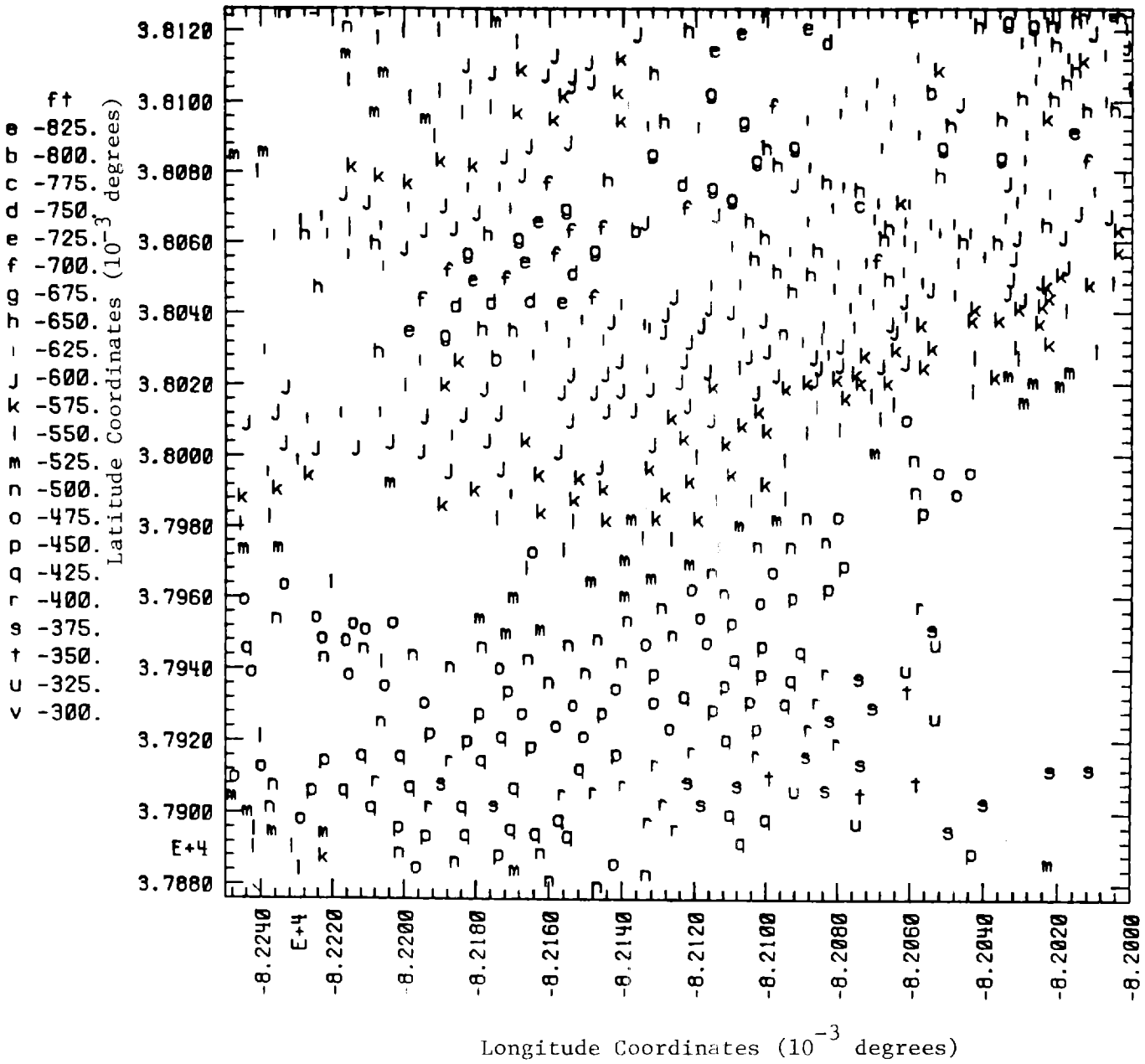

Figure 2. Data location of the top elevation of the Greenbrier Limestone. The axes x and y were expressed in unit of degree multiplied by 1000 and sign of x was changed in order to have correct map orientation. Negative elevations are below sea level.

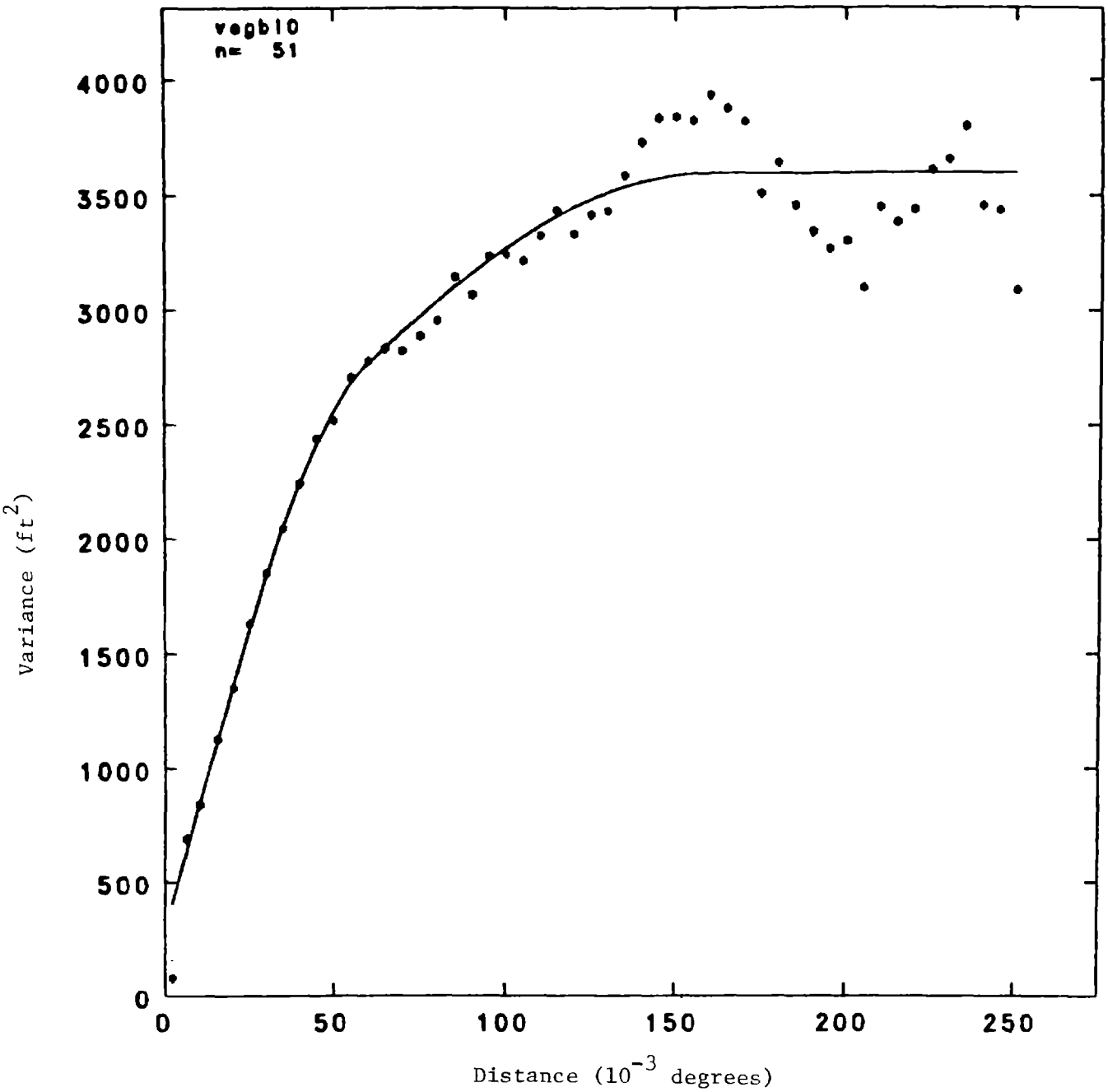

o1= 60.00, w1= 1500.00, c1= 300.00, mean= -49.4158, rms= 182.0438
o2= 160.00, w2= 1800.00, wc= 3600.00, mean= -49.4158, rms= 182.0438

Figure 3. Variogram of the bottom elevation of the Greenbrier Limestone.

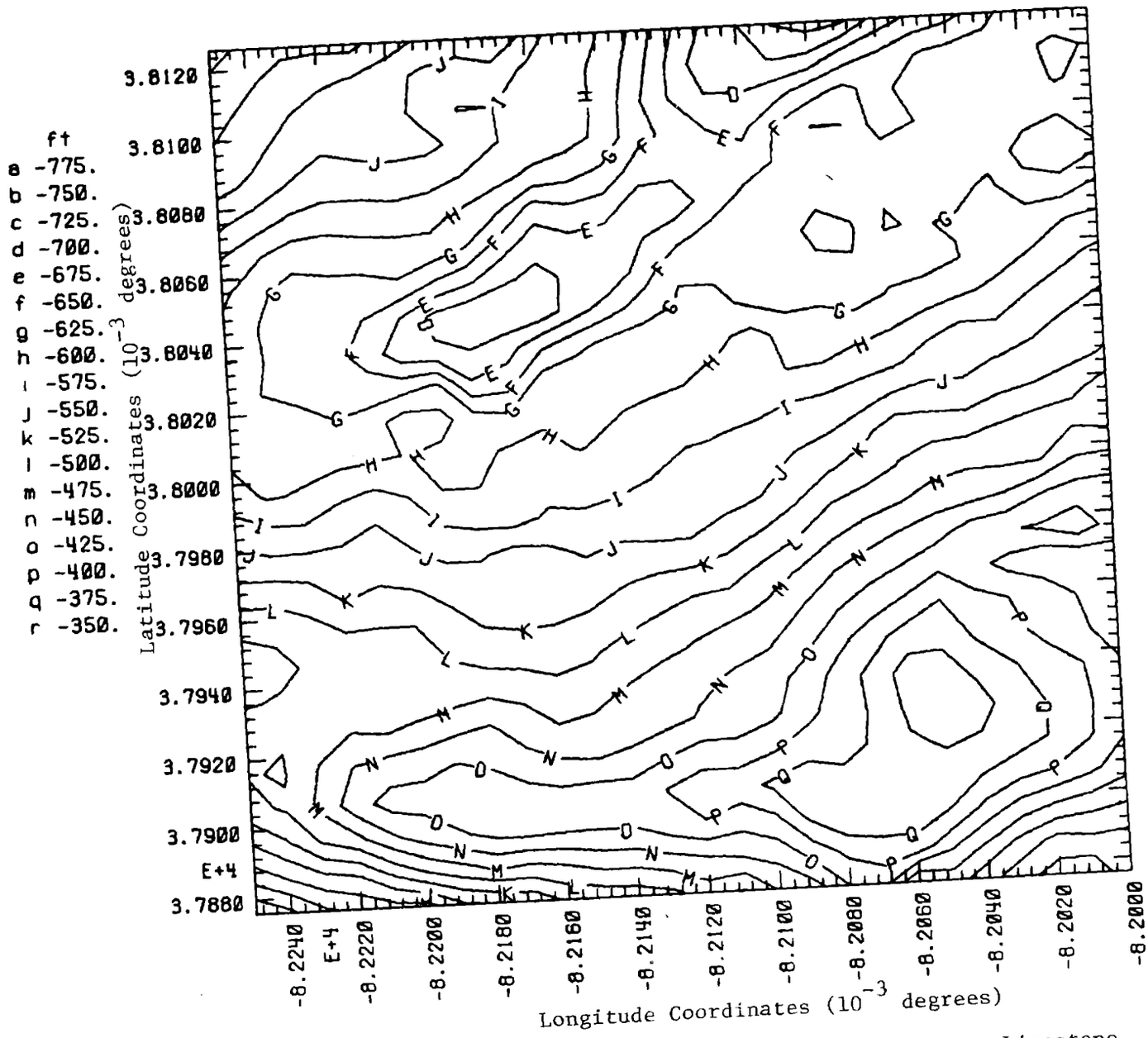

Figure 4. Kriged contour map of the top elevation of the Greenbrier Limestone. The axes x and y were expressed in unit of degree multiplied by 1000 and sign of x was changed in order to have correct map orientation. Negative elevations are below sea level.

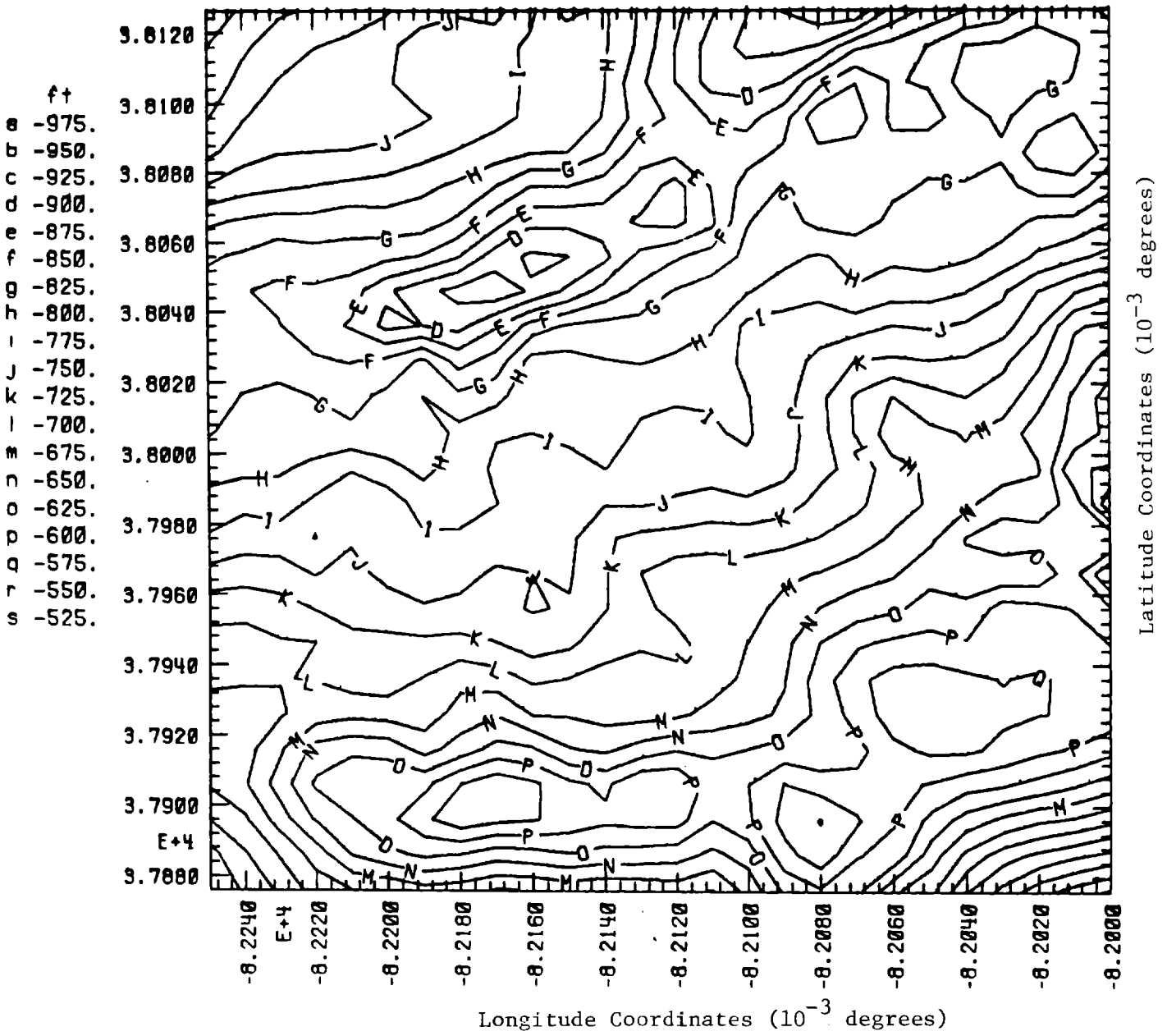

Figure 5. Kriged contour map of the bottom elevation of the Greenbrier Limestone. The axes x and y were expressed in unit of degree multiplied by 1000 and sign of x was changed in order to have correct map orientation. Negative elevations are below sea level.

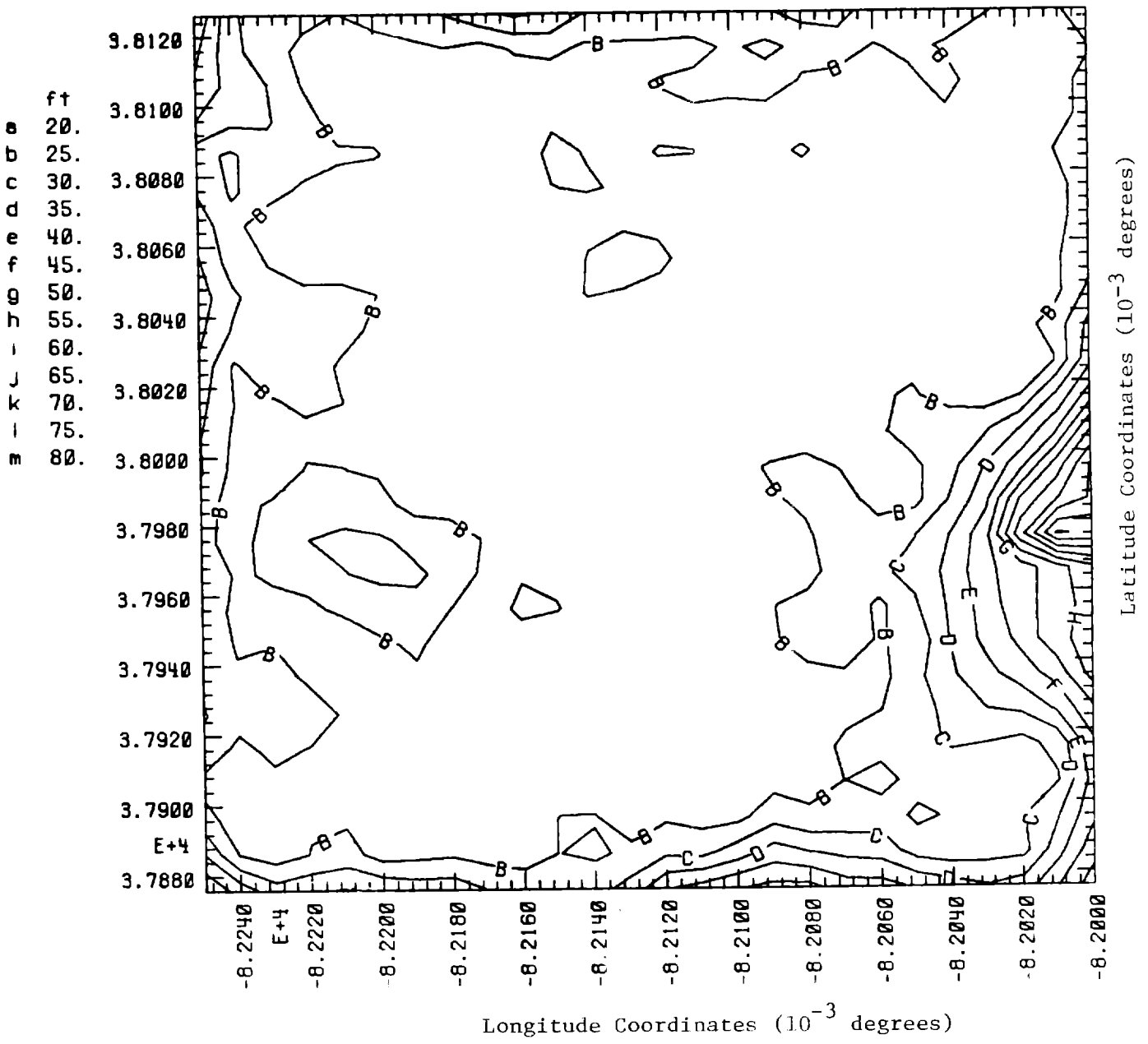

Figure 6. Uncertainty of estimates for the top elevation of the Greenbrier Limestone. The axes x and y were expressed in unit of degree multiplied by 1000 and sign of x was changed in order to have correct map orientation. The contour values represent one standard deviation.

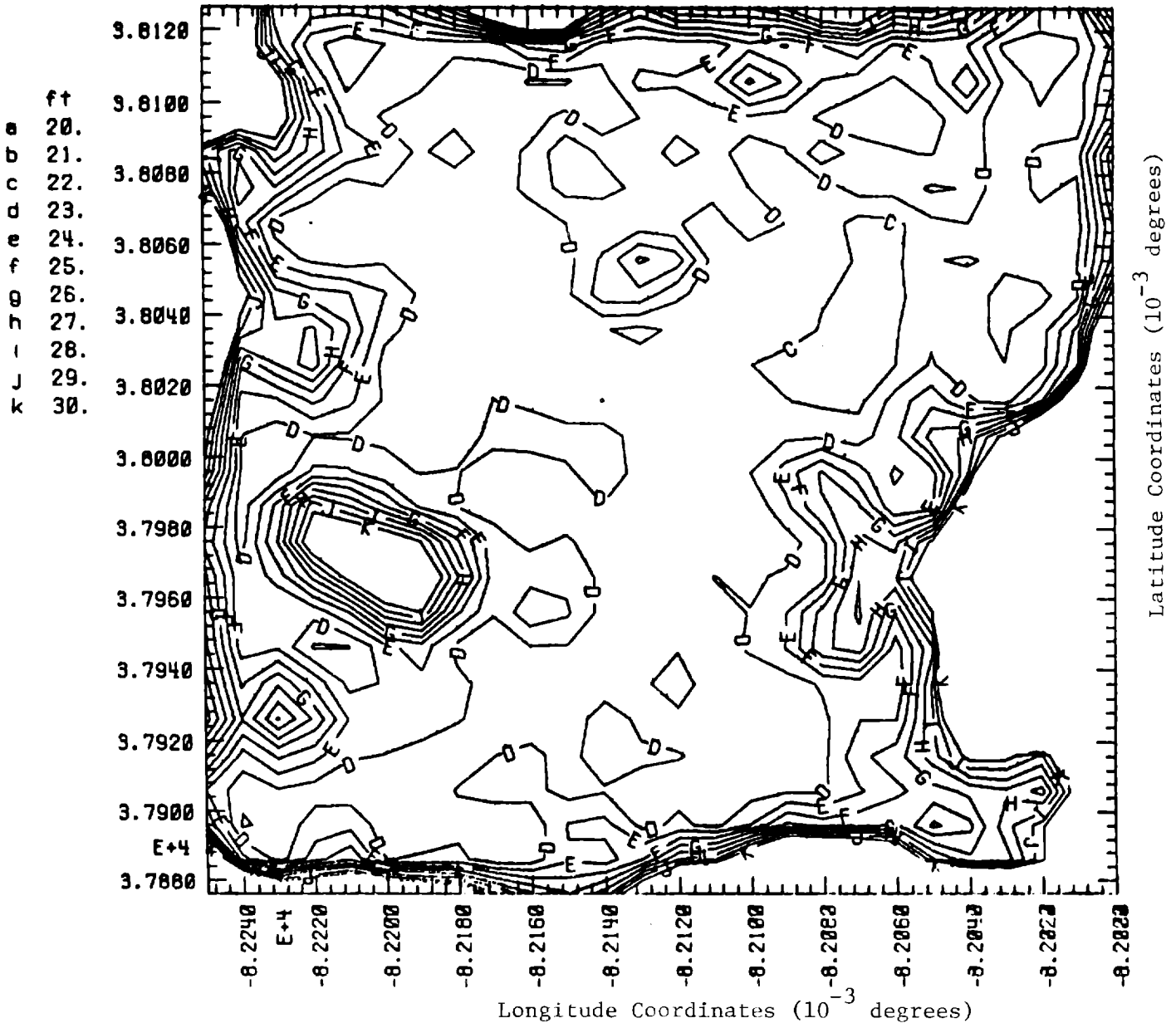

Figure 7. Uncertainty of estimates for the bottom elevation of the Greenbrier Limestone. The axes x and y were expressed in unit of degree multiplied by 1000 and sign of x was changed in order to have correct map orientation. The contour values represent one standard deviation.

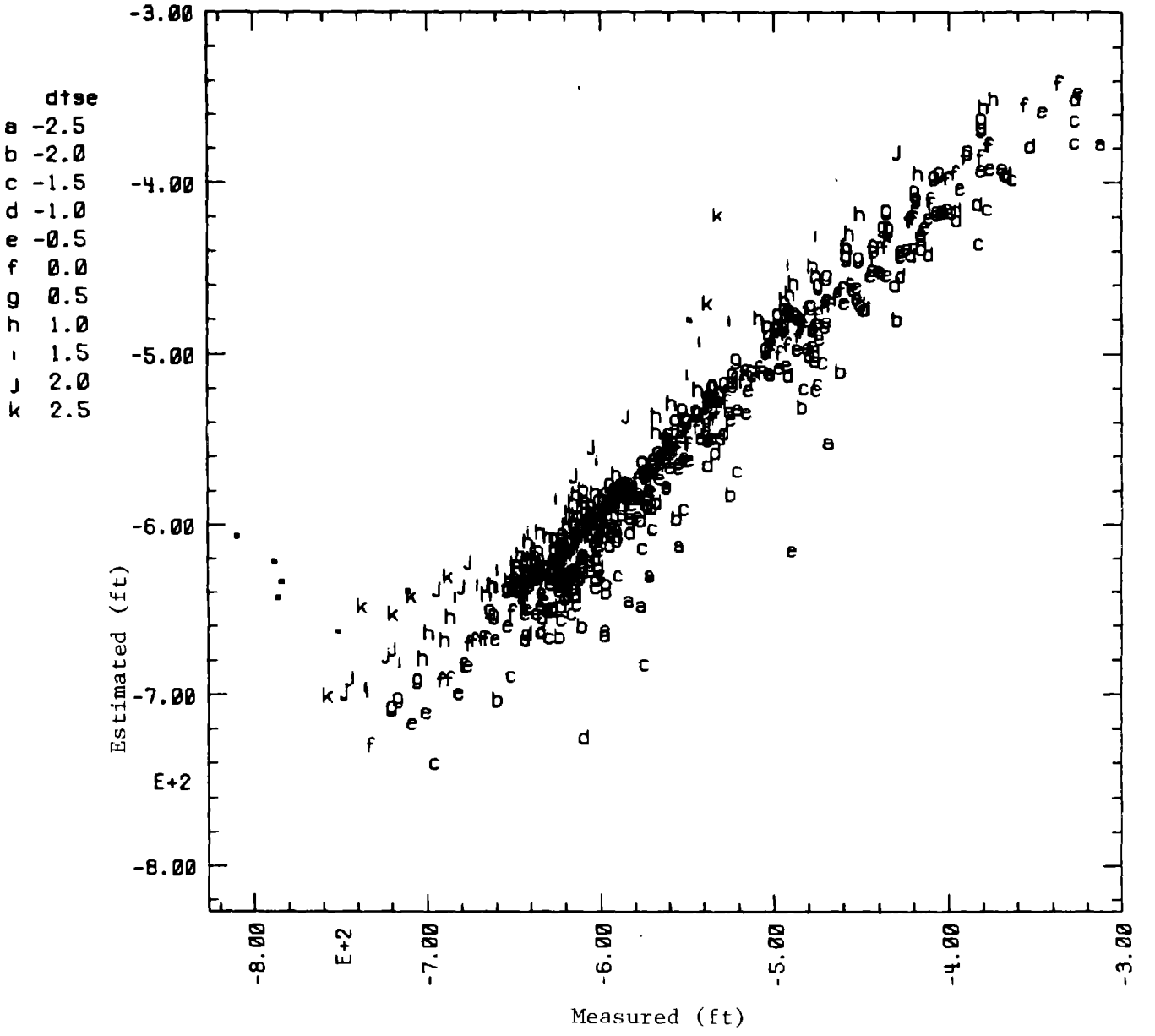

Figure 8. Measured vs estimated values for the top elevation of the Greenbrier Limestone. The estimated values are calculated from Thomas validation process; "dtse" is the doubting Thomas standard error defined on p. 3.

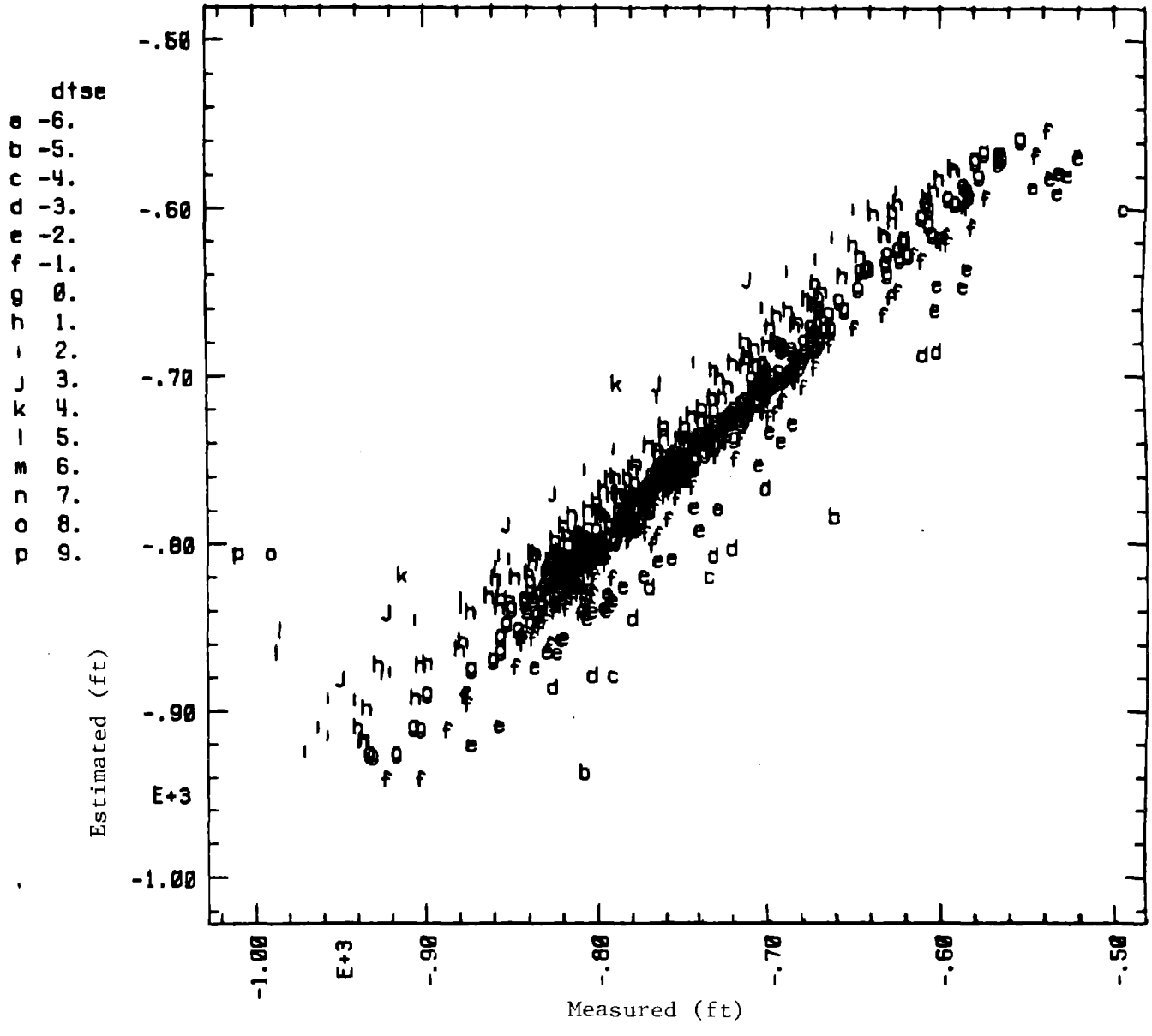

Figure 9. Measured vs estimated values for the top elevation of the Greenbrier Limestone. The estimated values are calculated from Thomas validation process; "dtse" is the doubting Thomas standard error defined on p. 3.

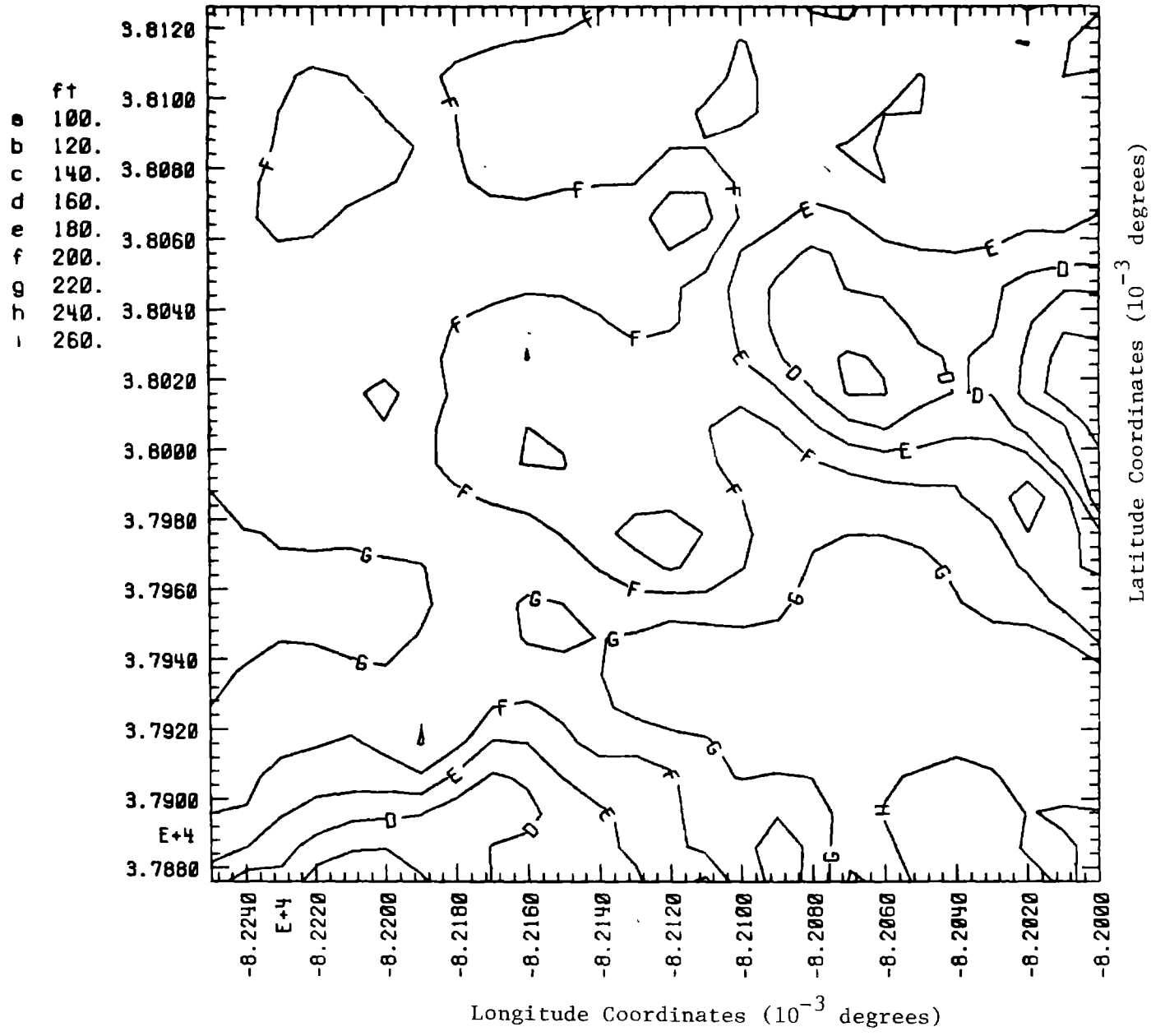

Figure 10. Kriged contour map of the thickness of the Greenbrier Limestone. The axes x and y were expressed in unit of degree multiplied by 1000 and sign of x was changed in order to have correct map orientation. Negative elevations are below sea level.

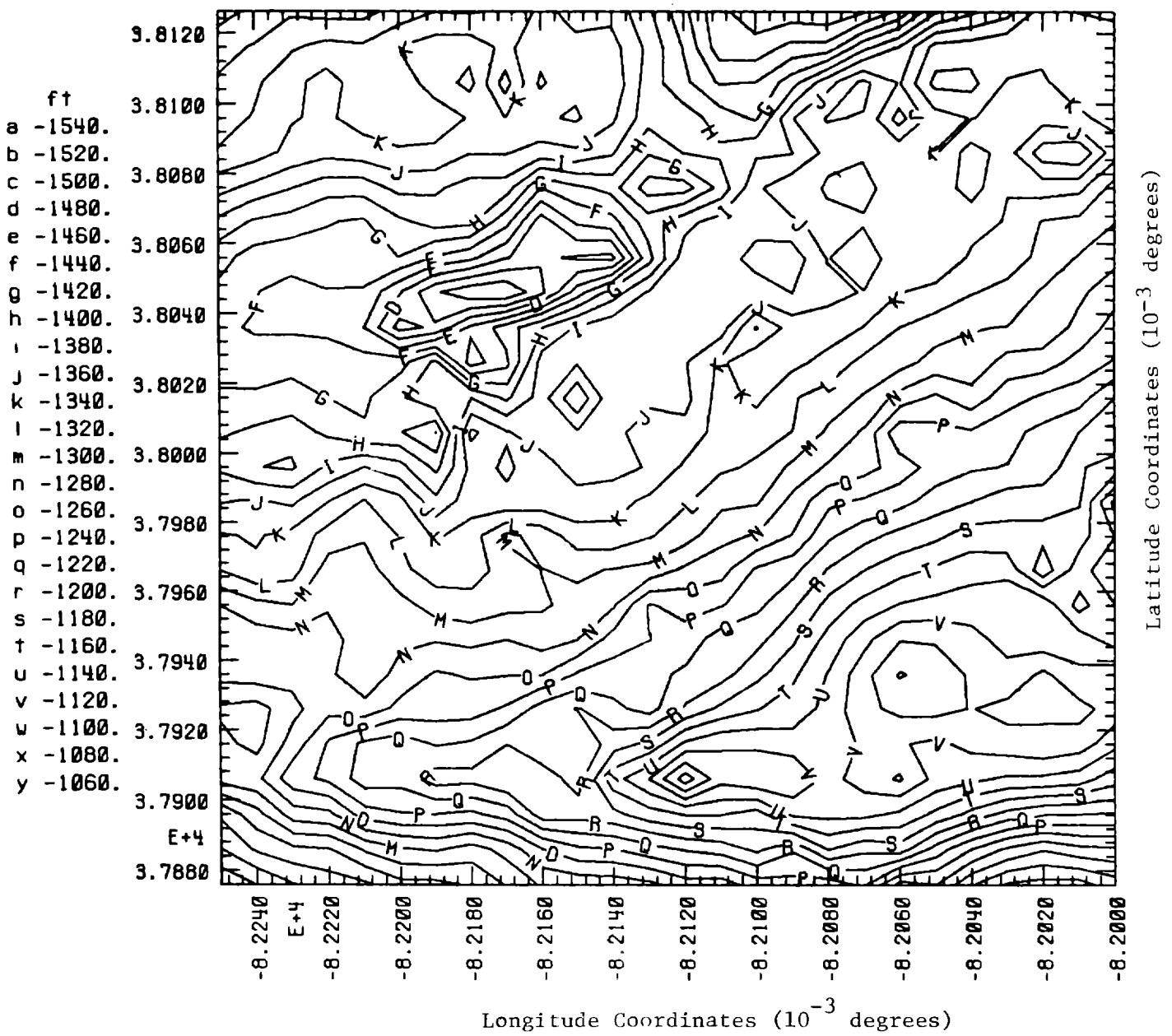

Figure 11. Kriged contour map of the top elevation of the Bera Sandstone. The axes x and y were expressed in unit of degree multiplied by 1000 and sign of x was changed in order to have correct map orientation. Negative elevations are below sea level.

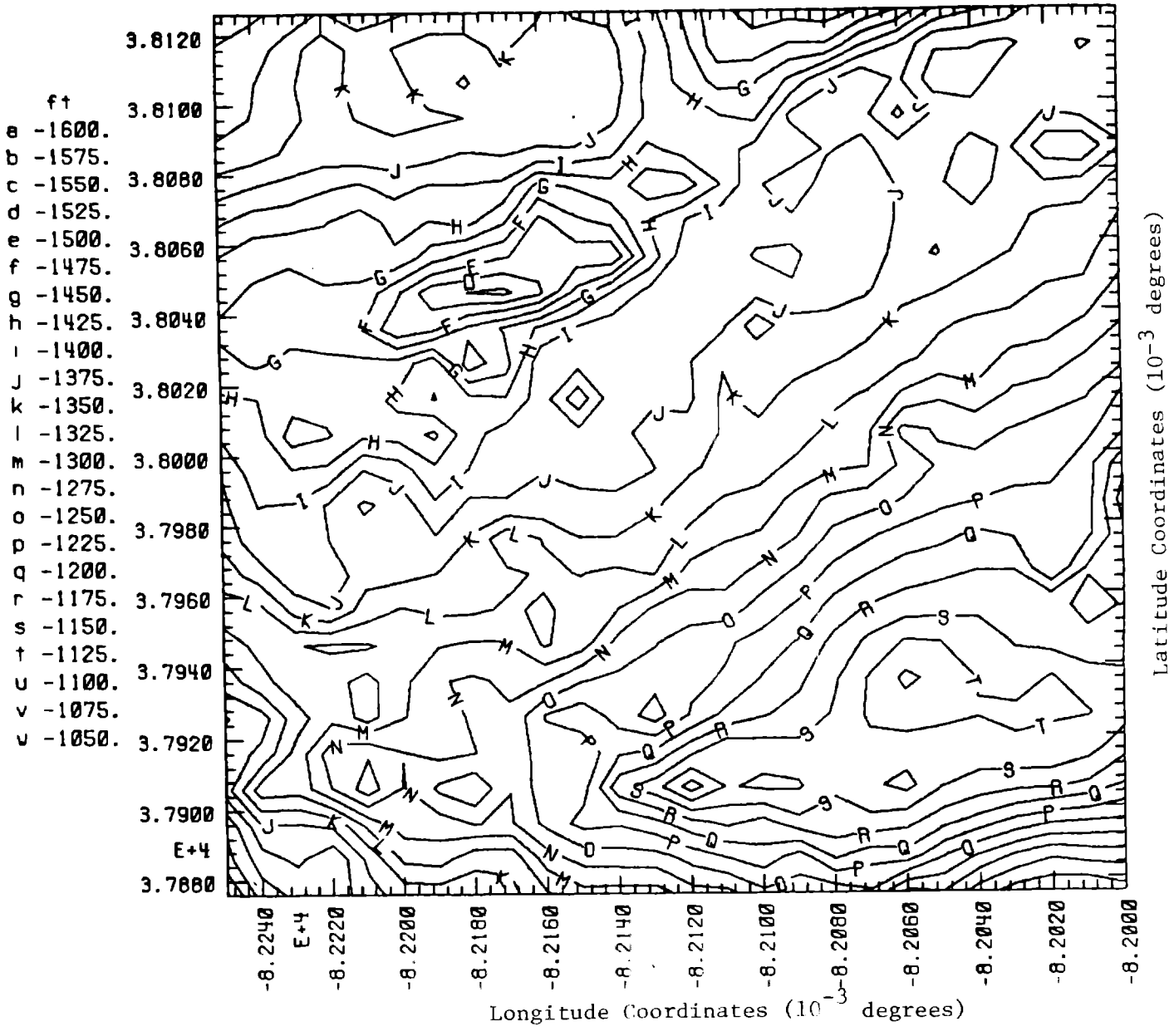

Figure 12. Kriged contour map of the bottom elevation of the Berea Sandstone. The axes x and y were expressed in unit of degree multiplied by 1000 and sign of x was changed in order to have correct map orientation. Negative elevations are below sea level.

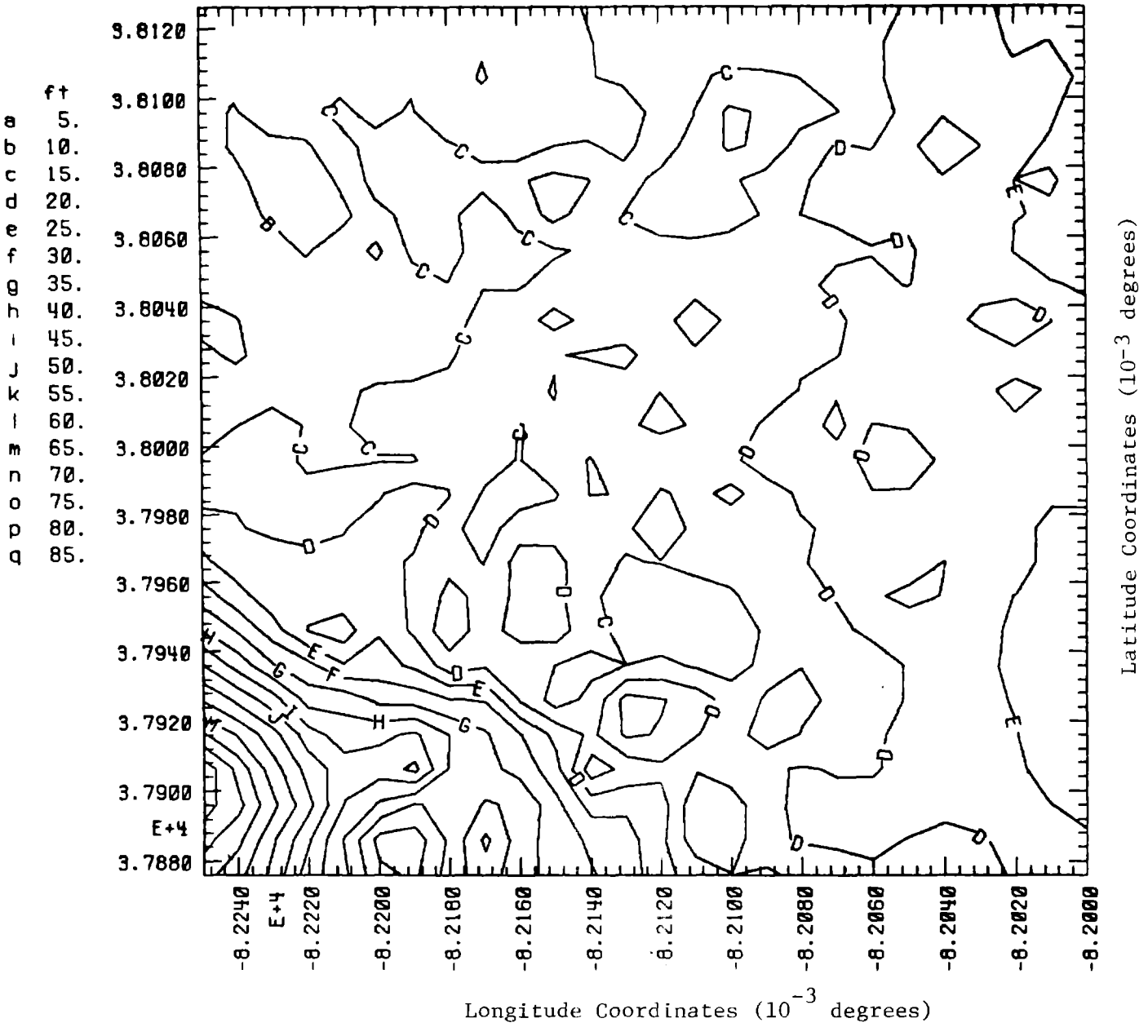

Figure 13. Kriged contour map of the thickness of the Berea Sandstone. The axes x and y were expressed in unit of degree multiplied by 1000 and sign of x was changed in order to have correct map orientation. Negative elevations are below sea level.

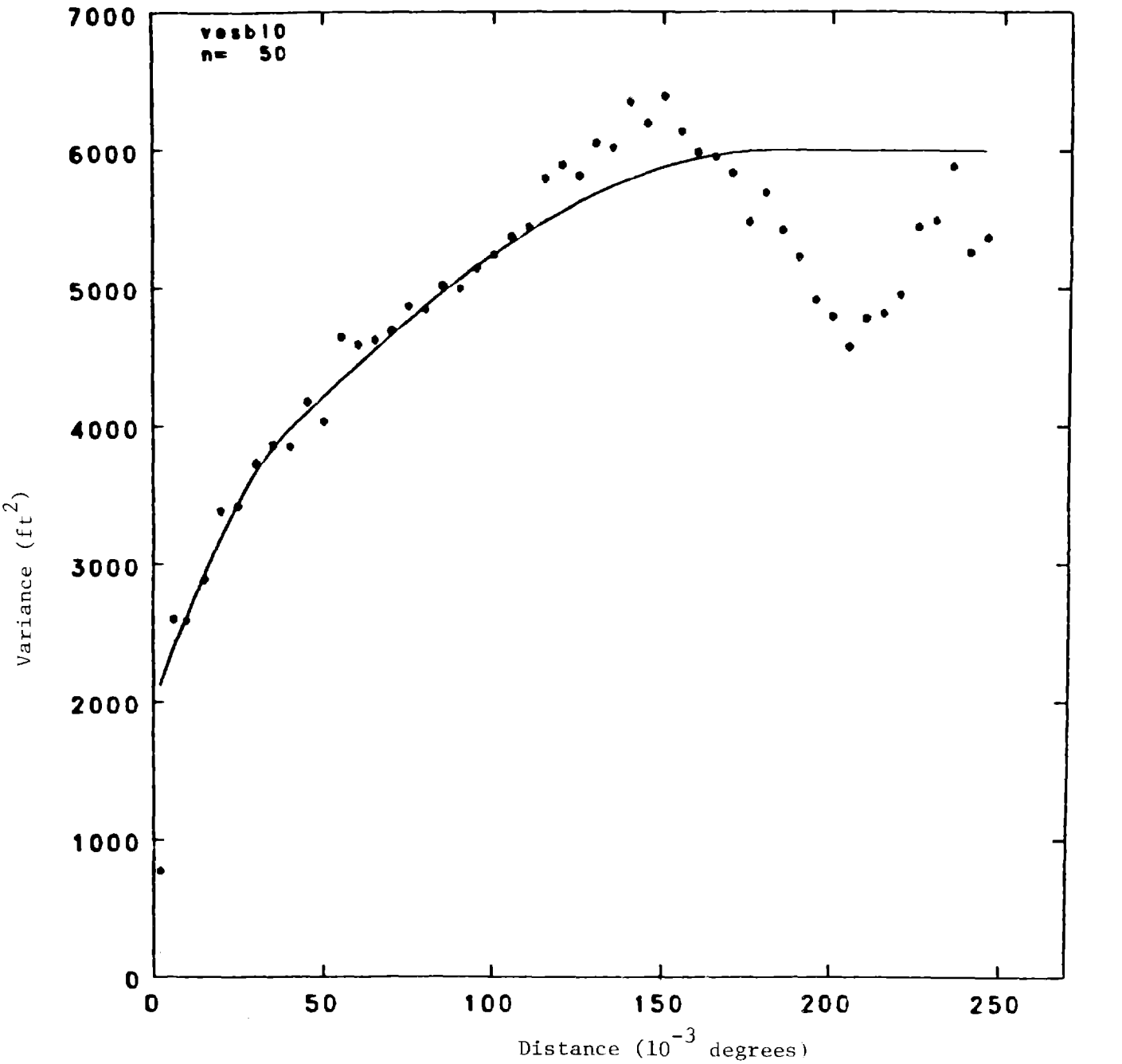

a1= 40.00, w1= 1000.00, c1= 2000.00, mean= -214.5821, rms= 555.2328
a2= 180.00, w2= 3000.00, wc= 6000.00, mean= -214.5821, rms= 555.2328

Figure 14. Variogram of the bottom elevation of the Devonian Shale (537 data).

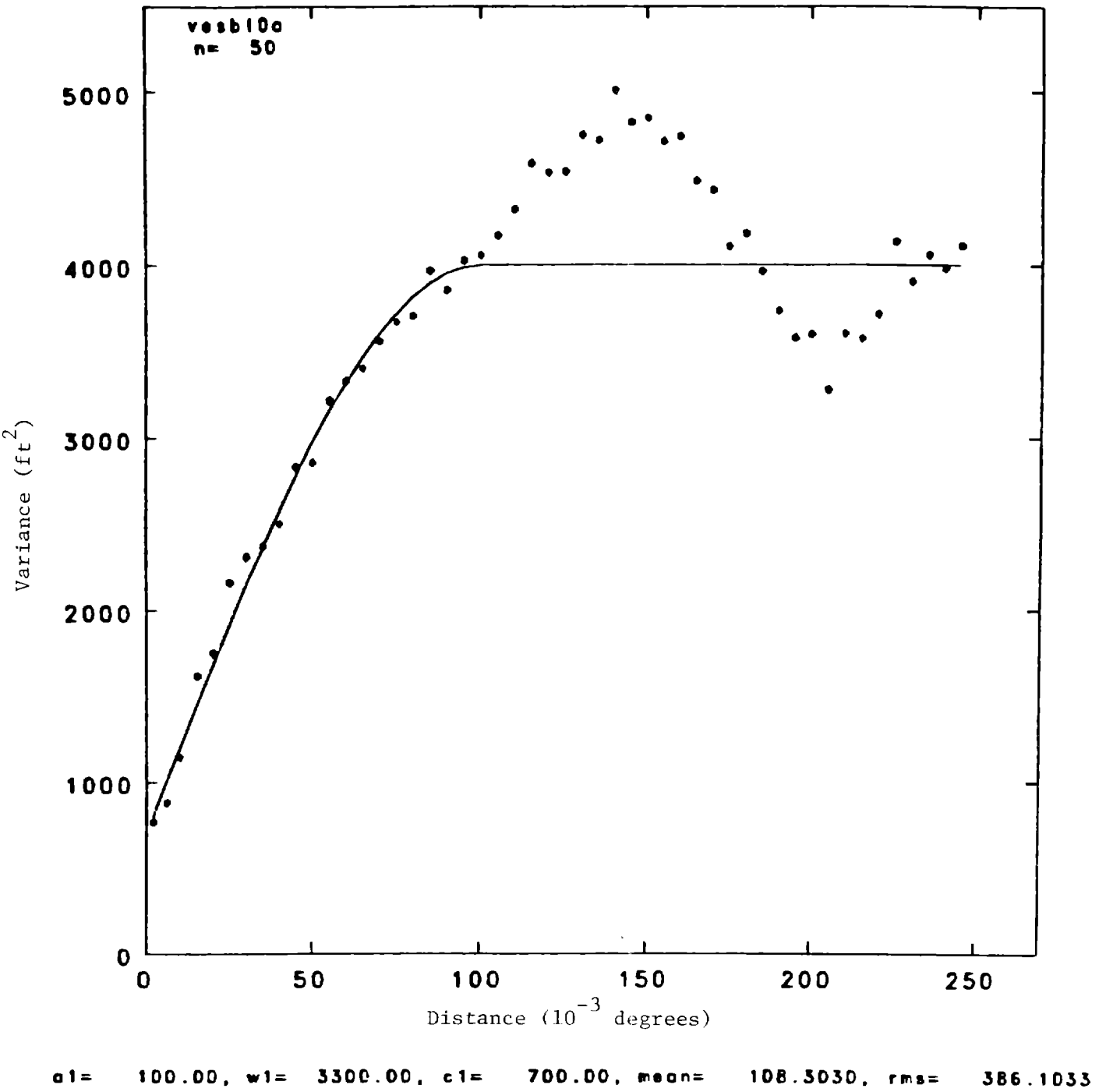

Figure 15. Variogram of the bottom elevation of the Devonian Shale (516 data).

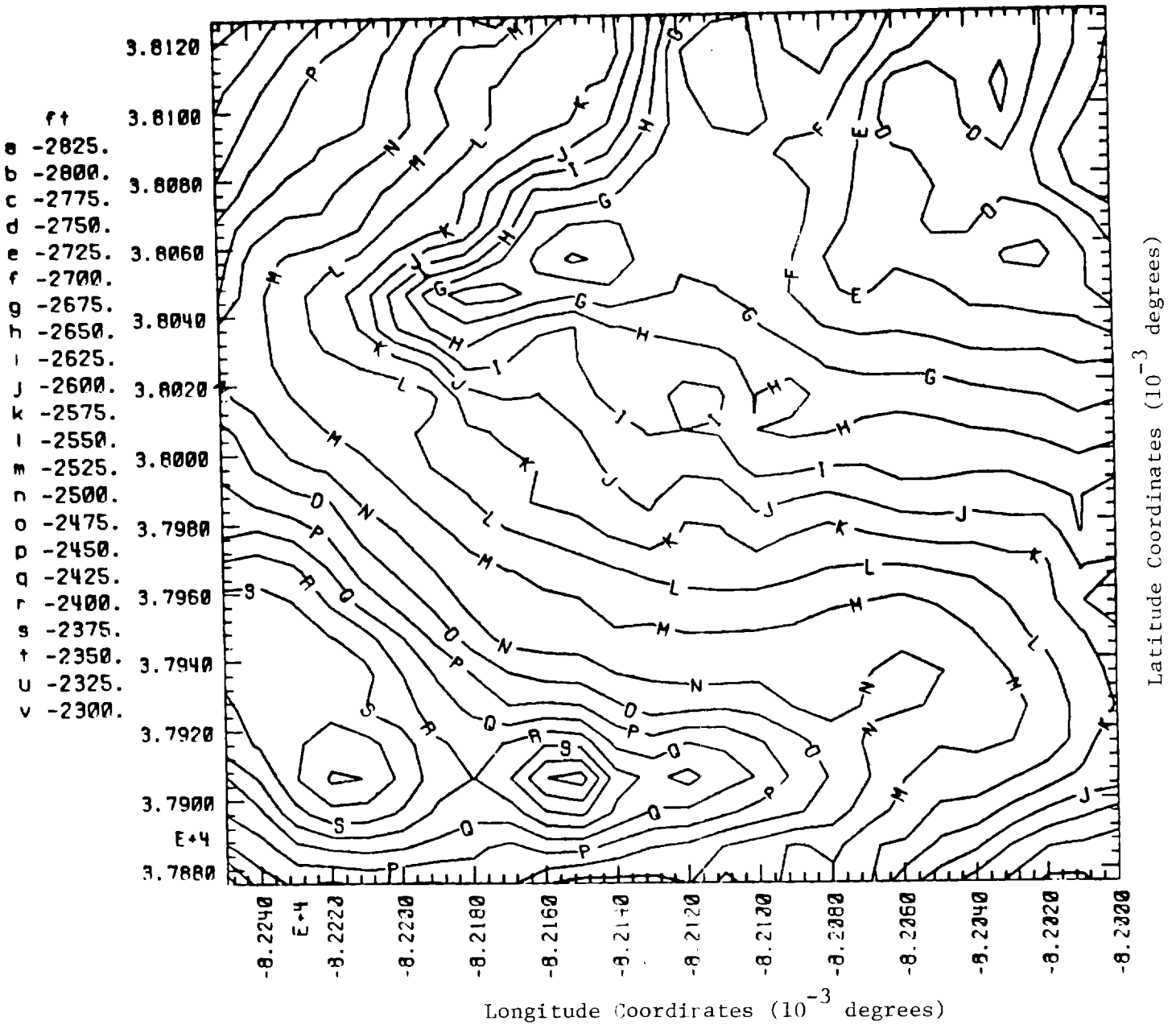

Figure 16. Kriged contour map of the bottom elevation of the Devonian Shale. The axes x and y were expressed in unit of degree multiplied by 1000 and sign of x was changed in order to have correct map orientation. Negative elevations are below sea level.

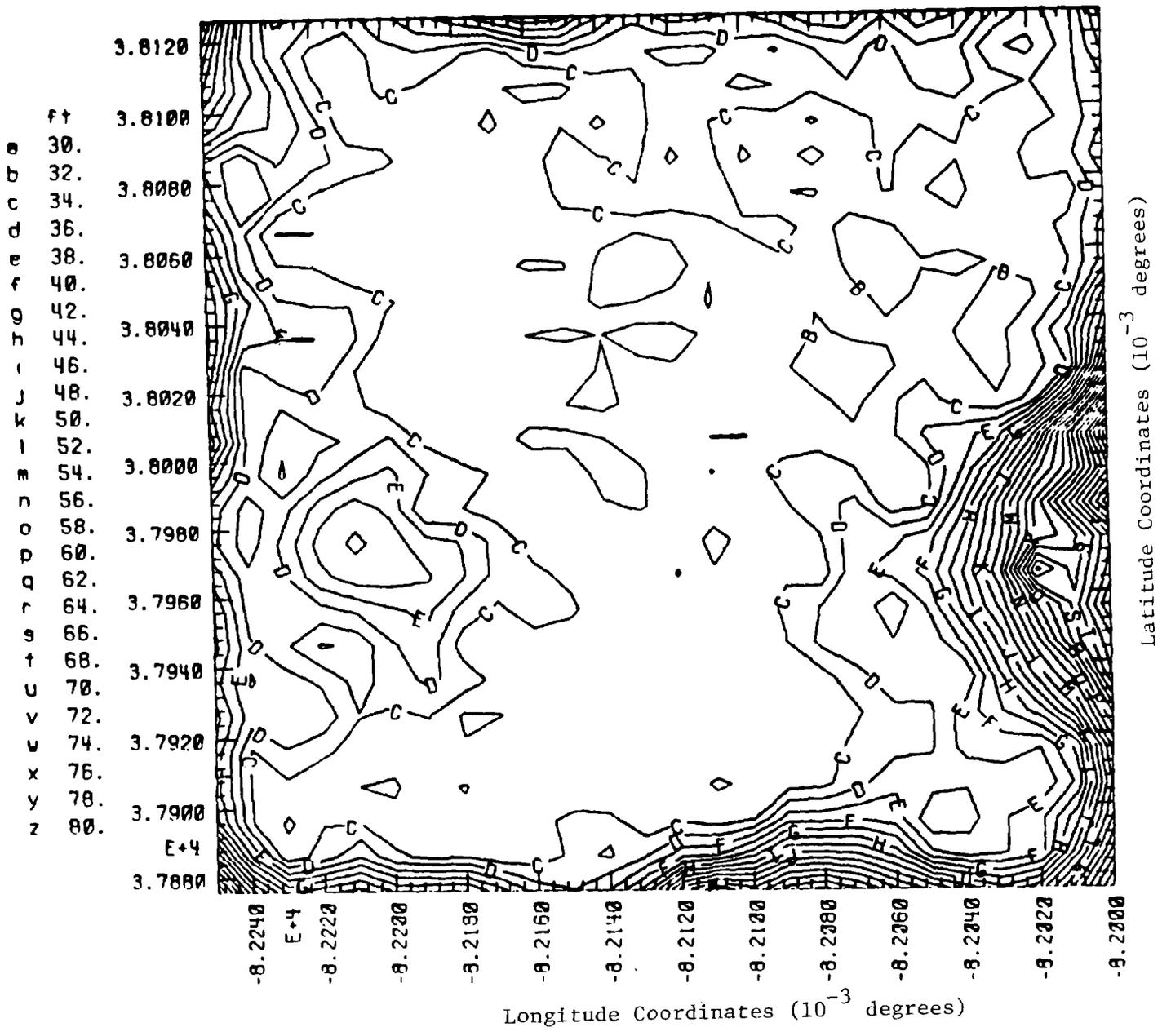

Figure 17. Uncertainty of estimates for the bottom elevation of the Devonian Shale. The axes x and y were expressed in unit of degree multiplied by 1000 and sign of x was changed to have correct map orientation. The contour values represent one standard deviation.

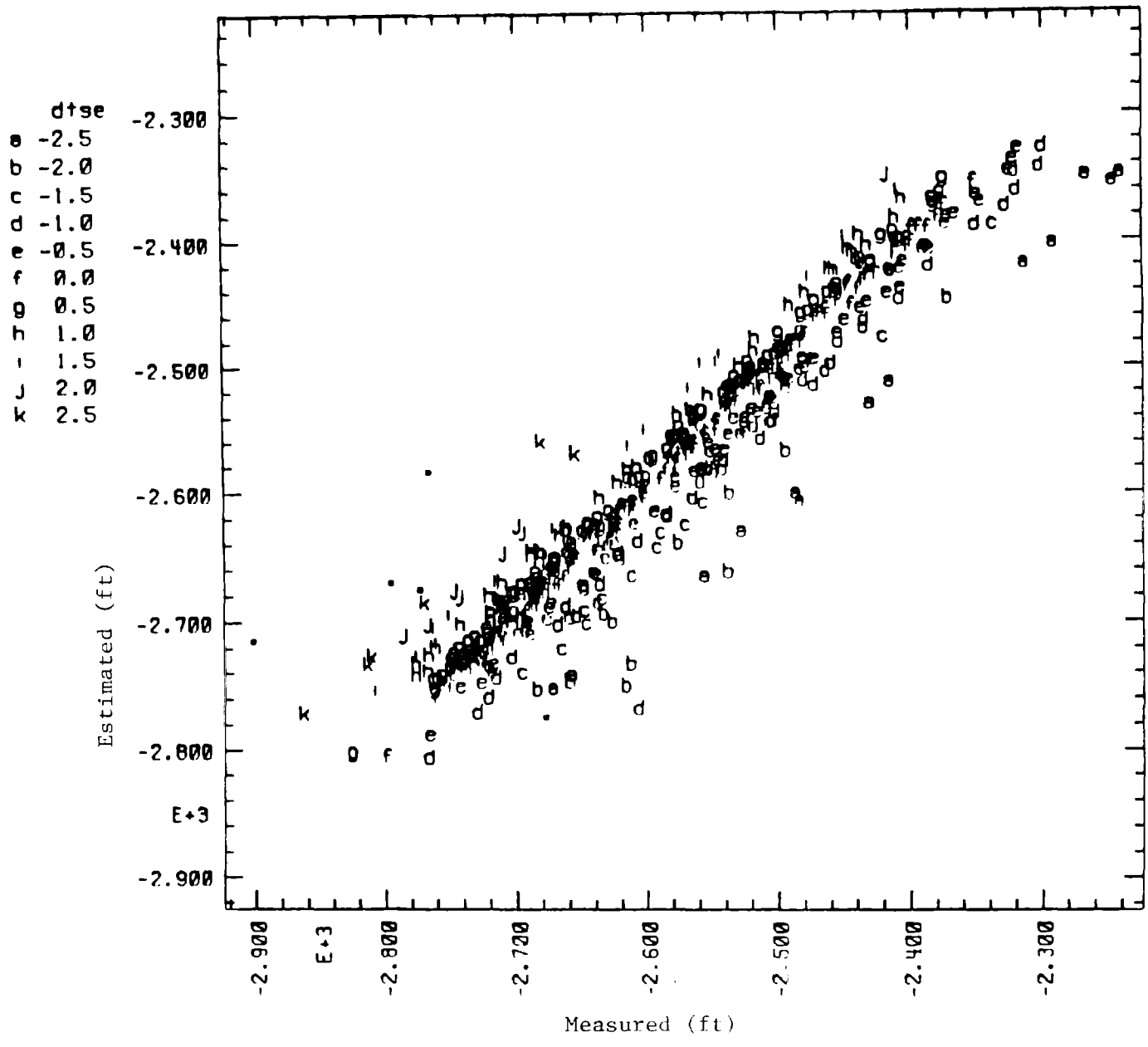

Figure 18. Measured vs estimated values for the bottom elevation of the Devonian Shale. The estimated values are calculated from Thomas validation process; "dtse" is the doubting Thomas standard error defined on p. 3.

4. ANALYSIS OF PRODUCTION DATA

4.1 Rock Pressure

There are 538 rock pressure data in the study area. These are the gas pressures 24 hours after shut-in. Their histogram (Figure 19) indicates that 95% of them are between 200 and 510 psi. Figure 20 shows the average variogram for rock pressures; it has a large nugget effect and a spherical model with a range of 70 units. Beyond this range there is little correlation among data points. Figure 21 shows the kriged contour map for rock pressures and Figure 22 is the associated uncertainty of the estimates. Because of the large nugget effect and relatively short range (as compared with geological data), no large structure is apparent. However the general trend of the Warfield anticline can still be seen and is associated with high rock pressures.

4.2 10-Year Cumulative Production Data

There are 448 ten year cumulative production (10 CUP) data points in the study area (Figure 23). The histogram shows a lognormal distribution (Figure 24). Therefore we studied the log of the ten year cumulative production (log(10 CUP)). Its distribution now becomes normal (Figure 25). Figure 26 shows the variogram of the residuals of a linear drift for log(10 CUP); it has a large nugget effect and a relatively short range of 80 units. The kriged contour map based on this model is shown in Figure 27 and its associated uncertainty is shown in Figure 28. Traces of a trend from geological structure can still be identified. It seems that the low log(10 CUP) data are general found in the vicinity of the Warfield anticline while high production data are located in the NW limb of the Warfield anticline, between the structural axes.

The majority of the wells were stimulated by explosives shooting. However 36 of them were subjected to hydrofracturing. We studied separately the data sets corresponding to the two kinds of stimulations and found no appreciable difference.

It is conceivable that the range of the variogram is a reflection of the average size of the gas fields in the study area.

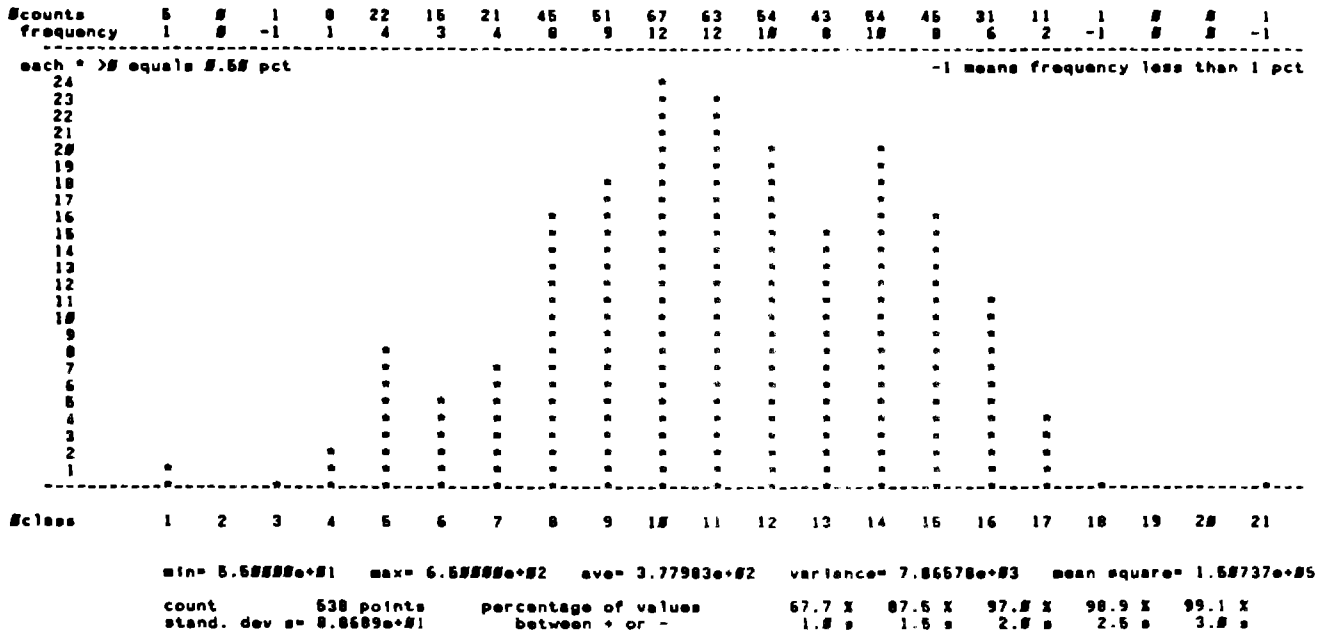

Figure 19. Histogram of rock pressures.

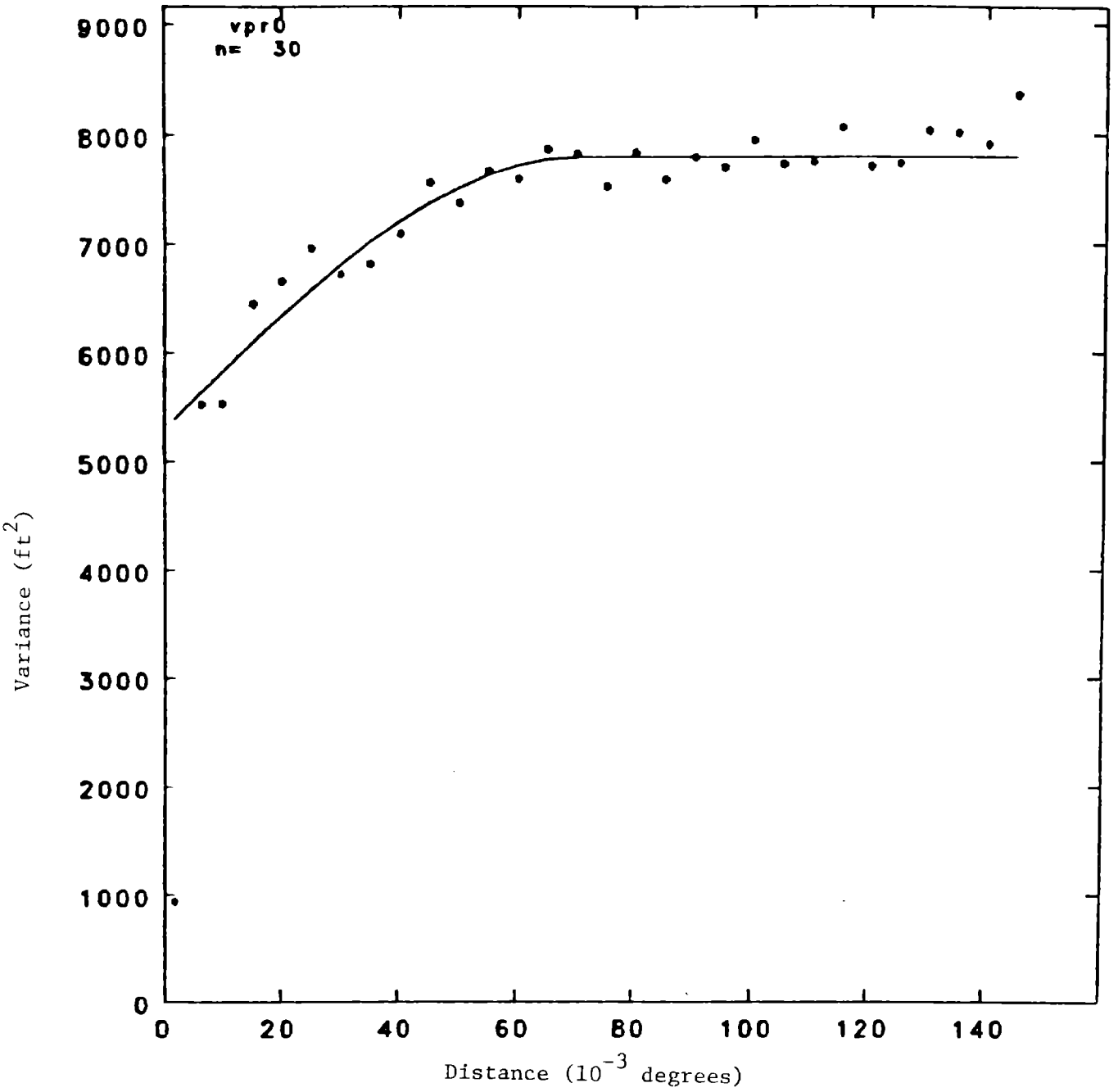

Figure 20. Variogram of rock pressures.

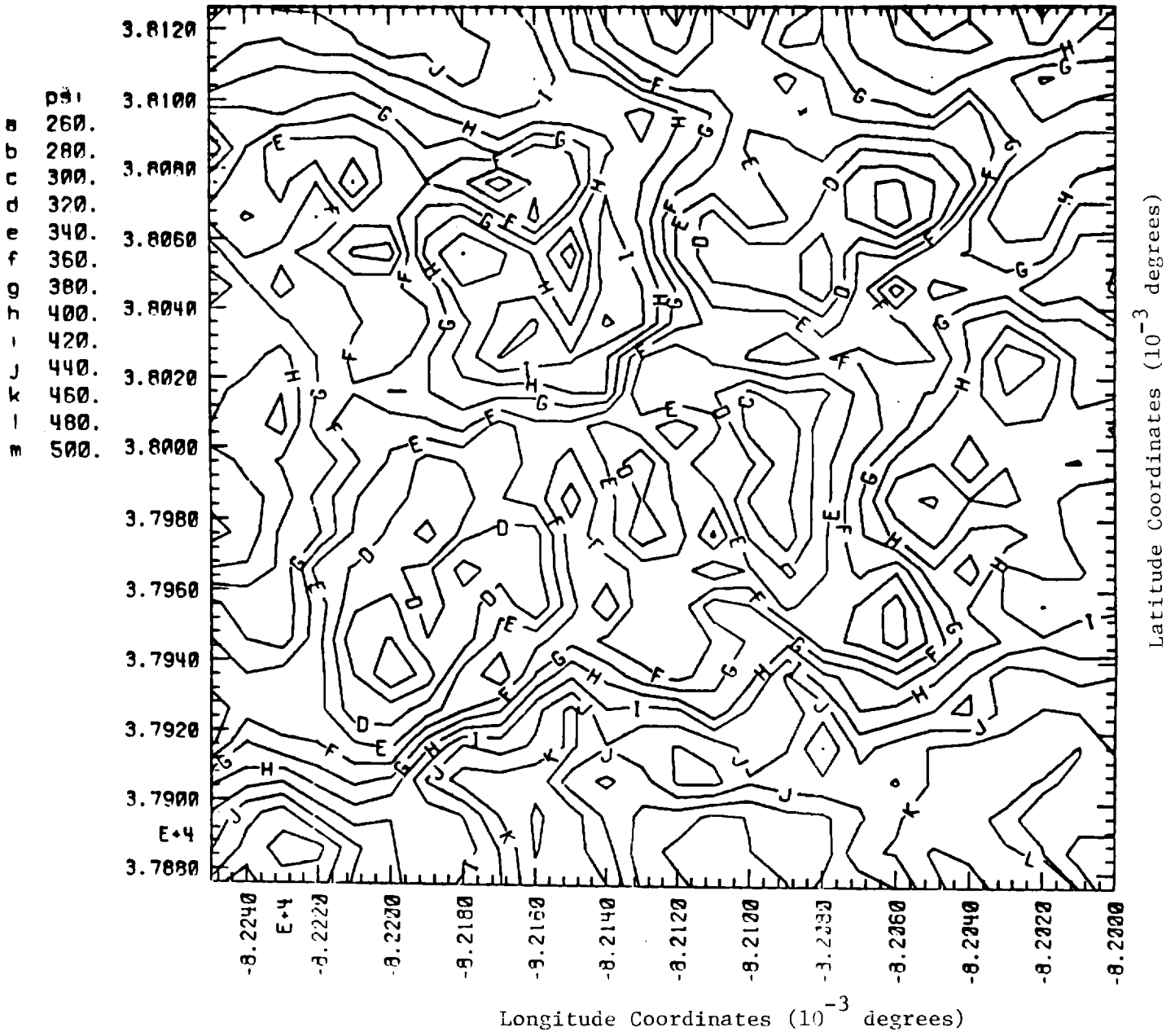

Figure 21. Kriged contour map of rock pressures, The axes x and y were expressed in unit of degree multiplied by 1000 and sign of x was changed in order to have correct map orientation.

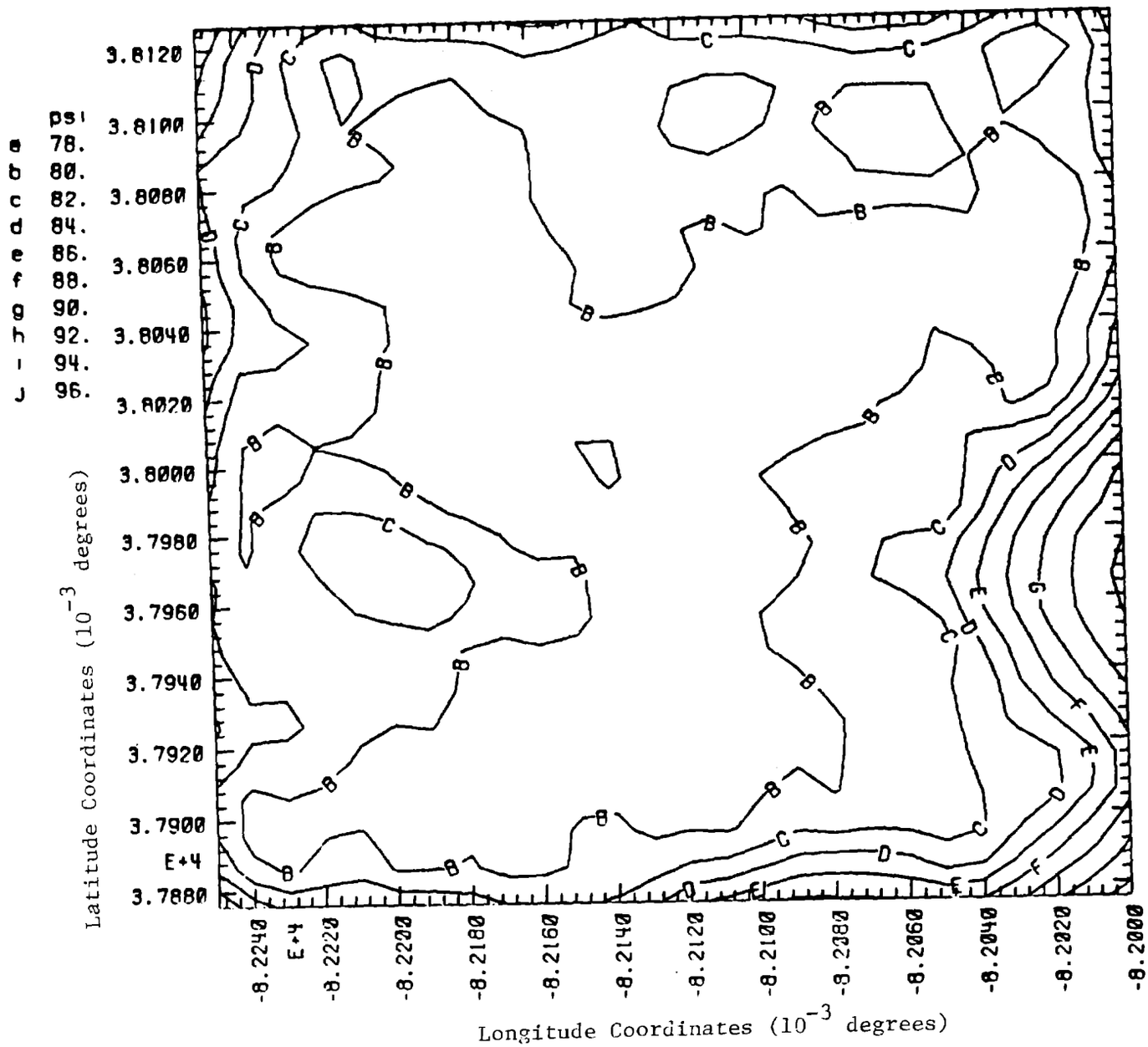

Figure 22. Uncertainty of estimates for rock pressures. The axes x and y were expressed in unit of degree multiplied by 1000 and sign of x was changed in order to have correct map orientation. The contour values represent one standard deviation

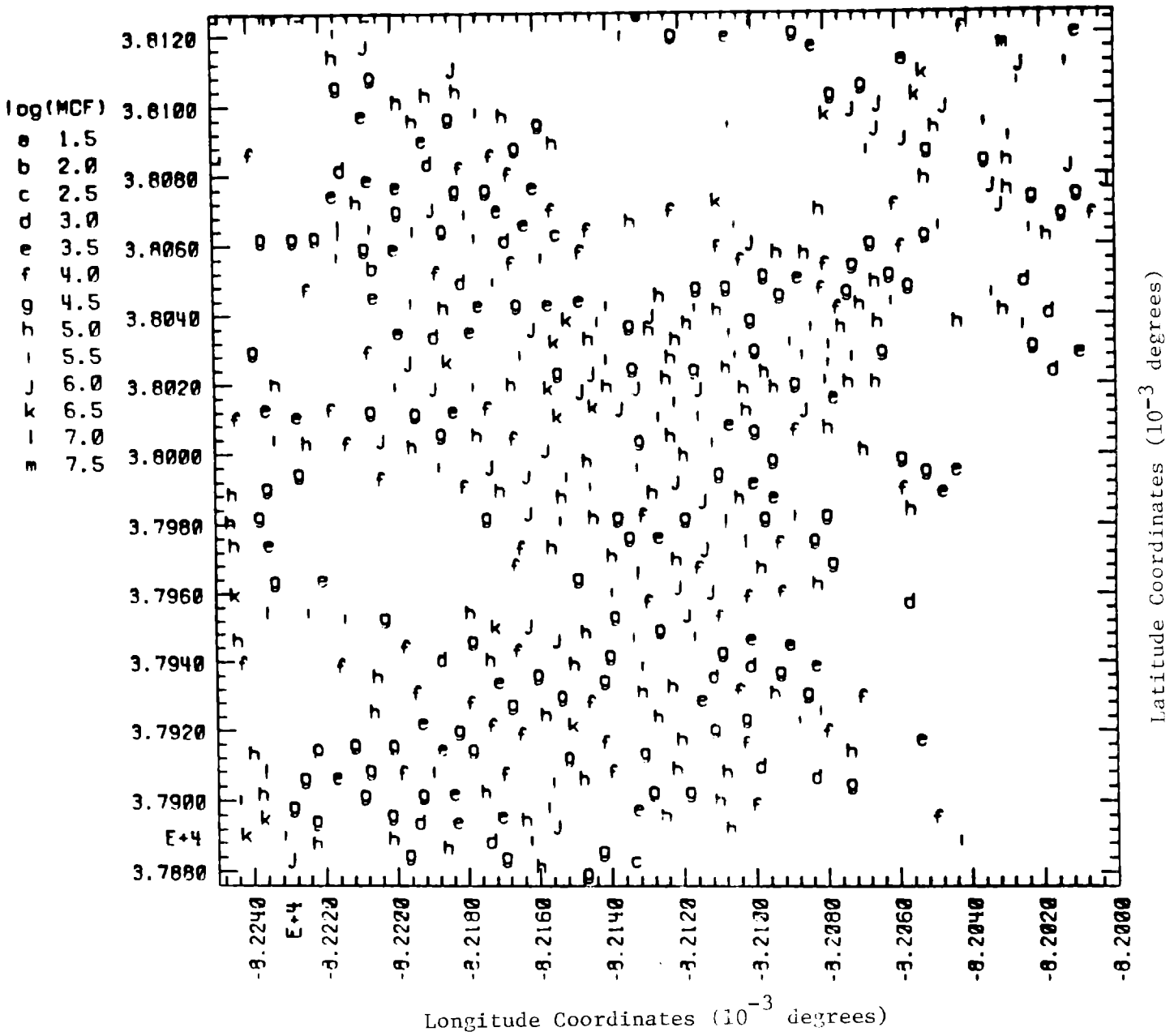

Figure 23. Location of data for the ten year cumulative production. The axes x and y were expressed in unit of degree multiplied by 1000 and sign of x was changed in order to have correct map orientation.

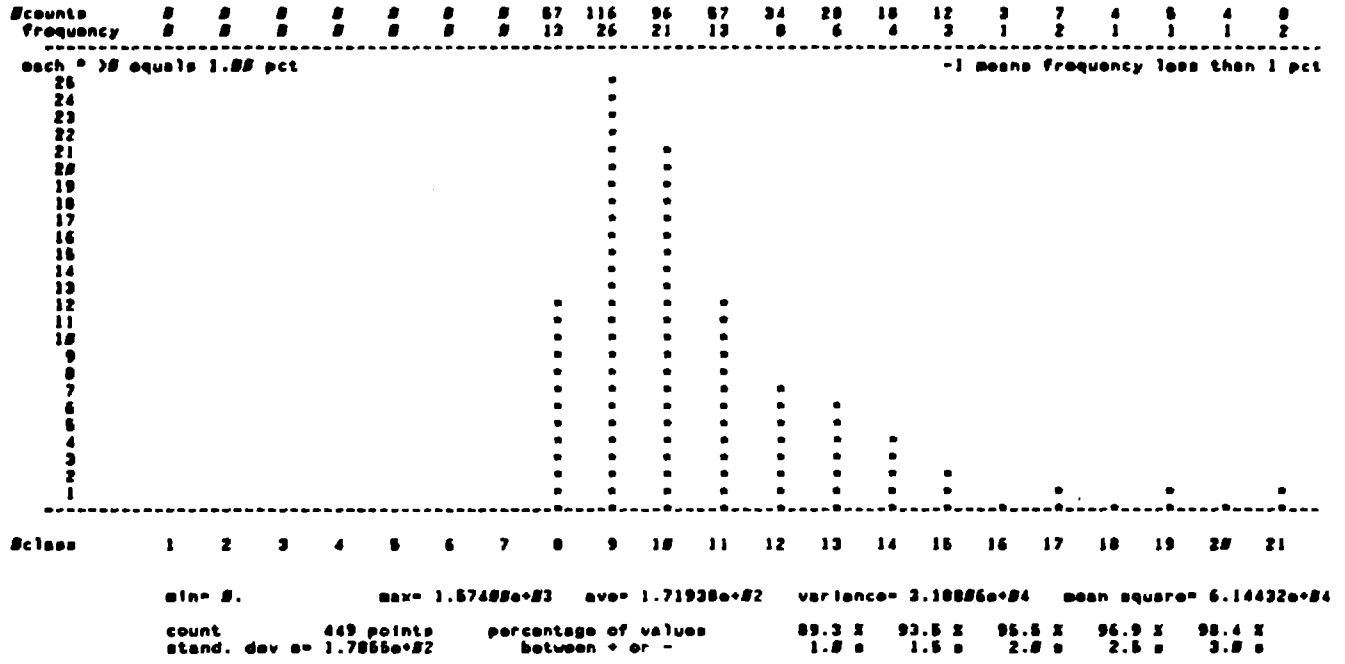

Figure 24. Histogram of ten year cumulative production.

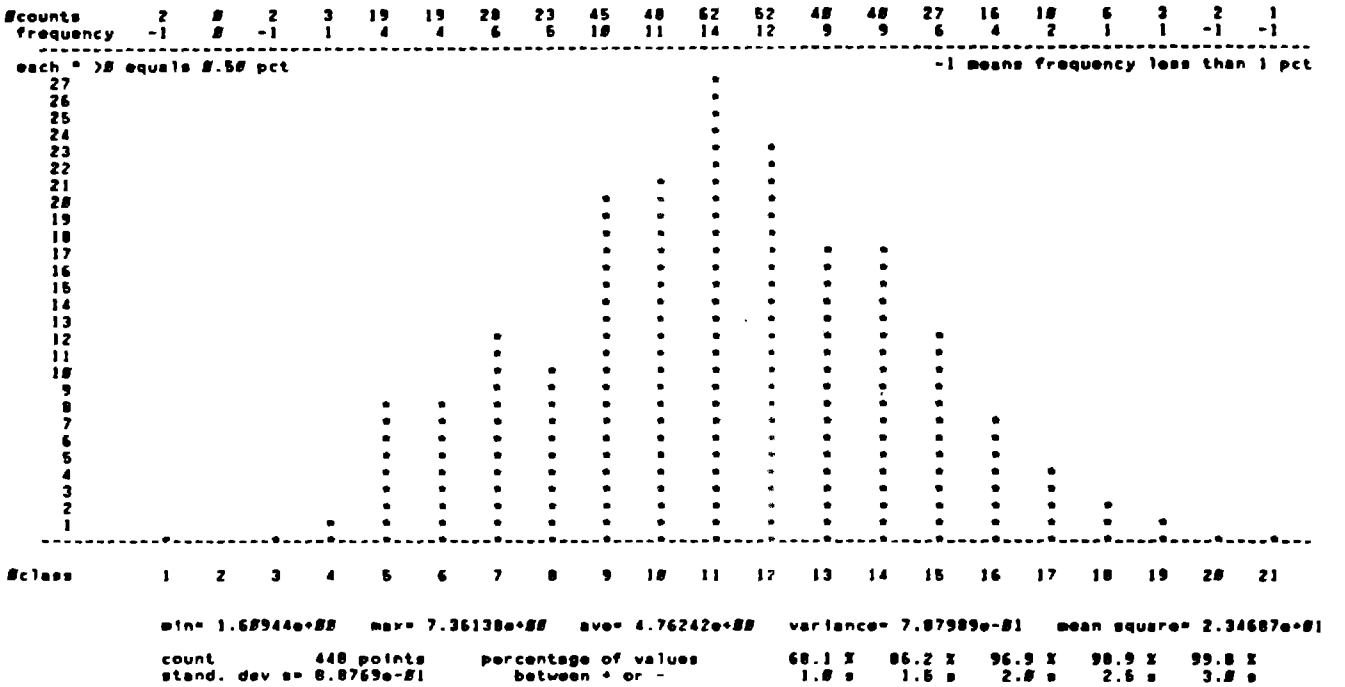

Figure 25. Histogram of the log of ten year cumulative production.

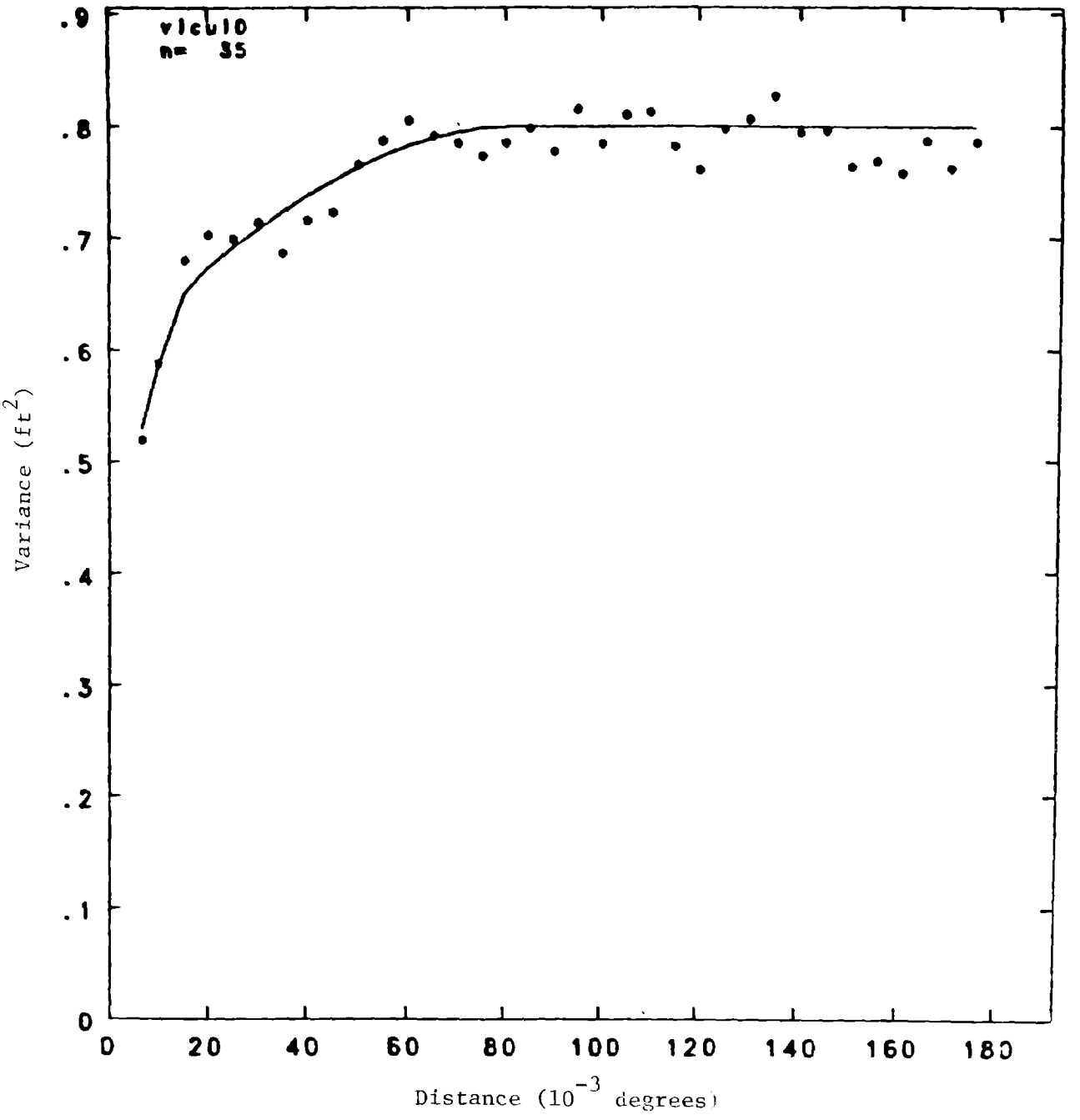

a1= 18.00, w1= 0.20, c1= 0.40, mean= -0.0104, rms= 0.0227
a2= 80.00, w2= 0.20, wc= 0.80, mean= -0.0104, rms= 0.0227

Figure 26. Variogram of the log of ten year cumulative production.

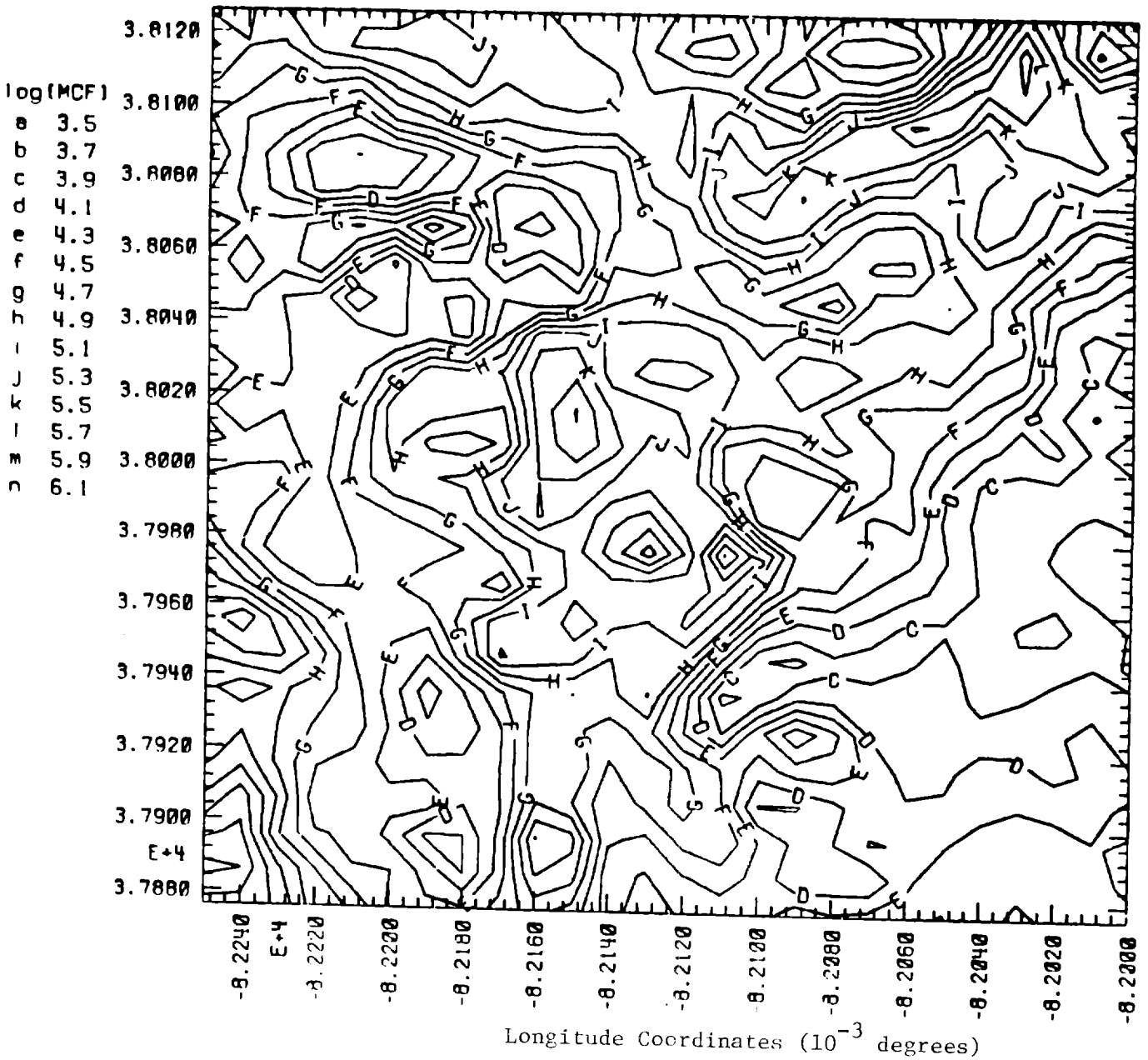

Figure 27. Kriged contour map of the log of ten year cumulative production. The axes x and y were expressed in unit of degree multiplied by 1000 and sign of x was changed in order to have correct map orientation.

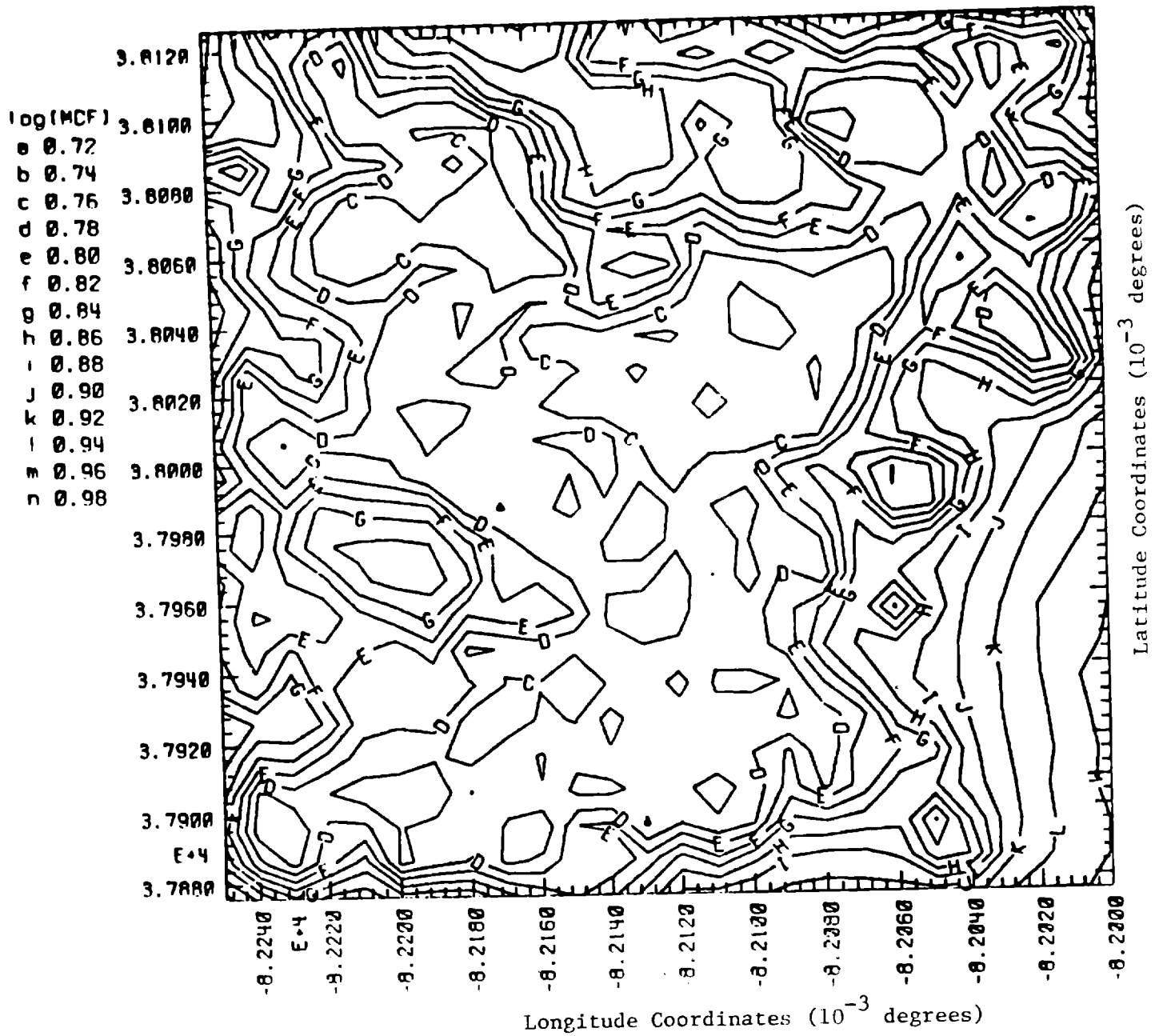

Figure 28. Uncertainty of estimates for the log of ten year cumulative production. The axes x and y were expressed in unit of degree multiplied by 1000 and sign of x was changed in order to have correct map orientation. The contour values represent one standard deviation.

5. SUMMARY

Geological and gas production data from southwestern West Virginia were analyzed by kriging. The geological structure does not change much with depth. The major structures are the Guthrie syncline in the north and the Warfield anticline in the south, with a general trend of N60°E. No apparent strong correlation between the geological and the production data was found. However both rock pressures and ten year cumulative production patterns appear somewhat related to the anticline structure. The spatial correlation of both rock pressures and ten-year cumulative production as shown in Figures 20 and 26 indicates that reasonable prediction of these parameters can be made within the study area (Figures 21 and 27). In contrast we also studied the open flow data and found little correlation. One possible explanation is that only a few wells were individually metered. If the observation from this study can be generalized to neighboring gas fields, it may provide some clues for future exploration strategy.

6. REFERENCES

Haught, O. L. (1968), "Structure Contour Map Datum Greenbrier Limestone in West Virginia", West Virginia Geological and Economic Survey.

Heuze, F.E. (1986), "The Unconventional Gas Program at Lawrence Livermore National Laboratory", UCID-20610, January.

Journel, A. G. and C. J. Huijbregts (1978), "Mining Geostatistics", Academic Press, New York, 600 P.

Mao, N. (1983), "Kriging of Geological and Physical Parameters from Yucca Flat, NTS", Lawrence Livermore National Laboratory UCID-19880.

Matheron, G. (1971), "The Theory of Regionalized Variables and Its Applications", Center for Mathematical Morphology, Paris School of Mines, Fontainebleau, France, No. 5, 211 p.

7. ACKNOWLEDGMENTS

This research was performed as a part of the LLNL Unconventional Gas Program, under Contract W-7405-ENG-48 with the U.S. Department of Energy. The author would like to thank S. Pratt and C. Komar of METC for providing the data base and associated information for this study and F. Heuze, LLNL, and A. Yost, METC, for reviewing the manuscript.